GEAR TECHNOLOGY

The Journal of Gear Manufacturing

NOVEMBER/DECEMBER 1988

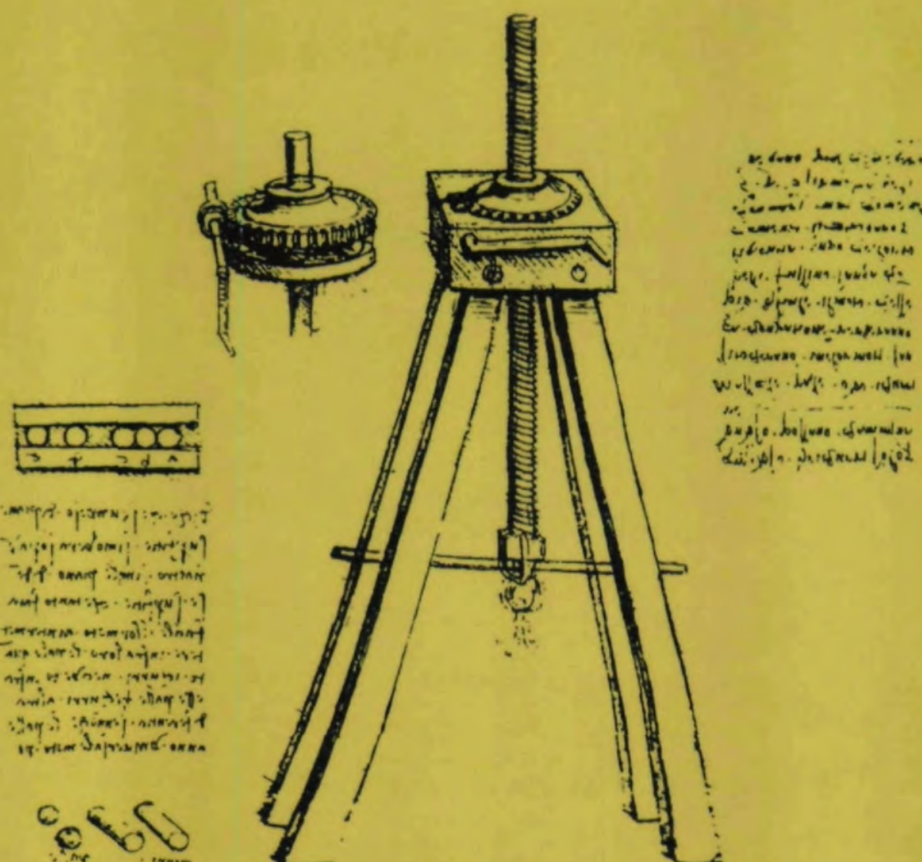

Improved Worm Gear Performance With Colloidal MoS_2-Containing Lubricants

Gear Tooth Profile Determination

Theory For The Synthesis Of Rotation Neutralizers

Basic Spur Gear Design

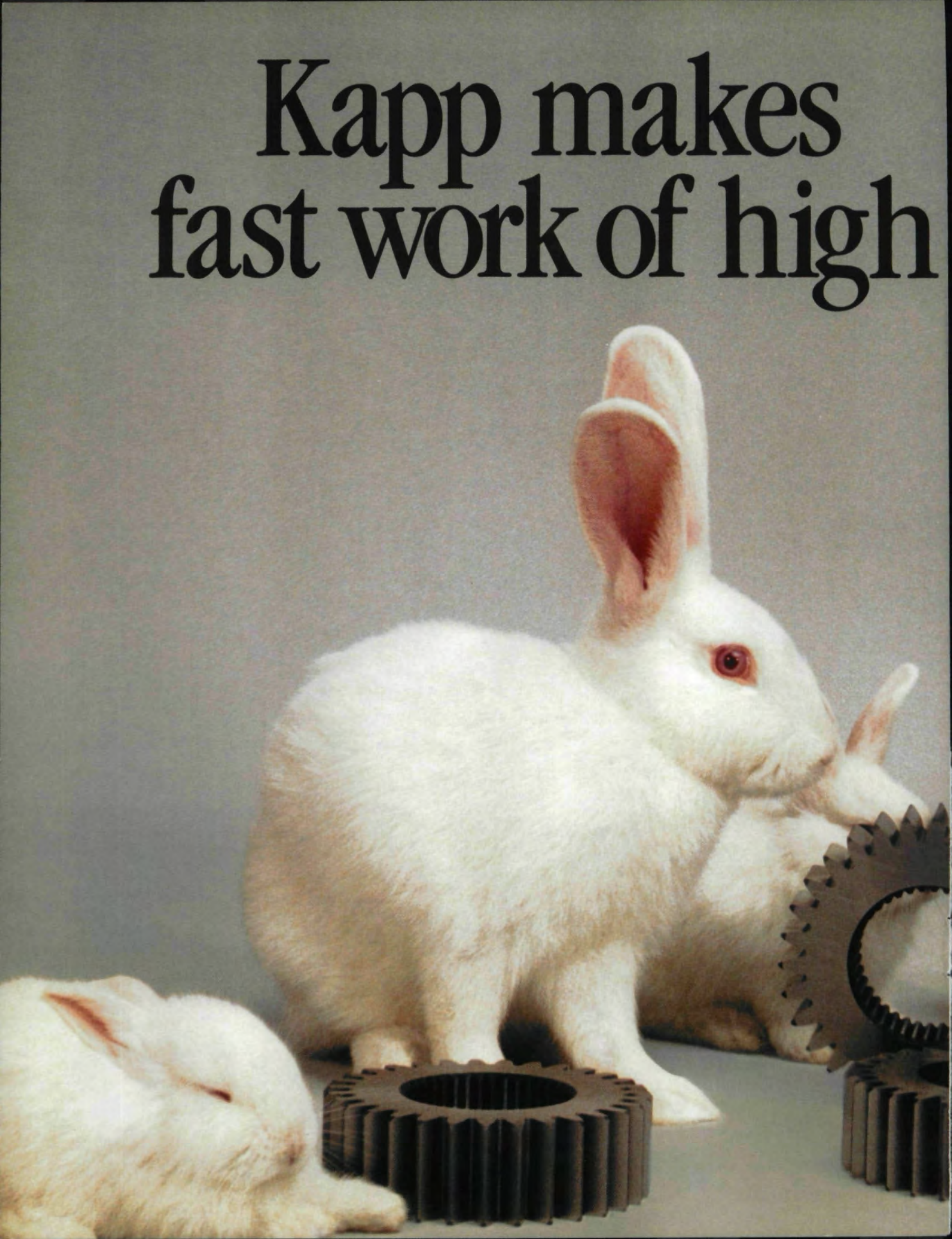
Kapp makes
fast work of high

production jobs.

High production cutting of identical gear shapes requires both speed and accuracy. But some fast, accurate machines incur maintenance and operator costs that eat up profits. With Kapp CBN form grinding, you don't give up productivity to maintain profitability.

- Kapp CBN machines are faster than other grinding processes, with no heat checking or burning. Kapp CBN accuracy has proven itself on spur & helical involute forms, radial forms, near-net forgings, internal & external profiles, vane pump slots and constant velocity joints.
- Kapp CBN machines are operator friendly, for fast recall of setups and accuracy time after time.
- Kapp CBN machines use CBN wheels that incorporate the desired form right in the wheel with no need for dressing.

If you'd like to find out how Kapp CBN technology can improve your productivity, contact American Pfauter, 925 Estes Ave., Elk Grove Village, IL 60007. Phone (312) 640-7500.

Mitsubishi Shapes the World of Gears...

What can Mitsubishi do for you? Mitsubishi can support you in all fields of gear manufacturing technology. Mitsubishi builds gear hobbers, gear shapers and gear shavers. All CNC controlled. Mitsubishi not only builds gear machinery but also manufactures various kinds of cutting tools. TiN coated gear hobs, shaping cutters and shaving cutters, etc. With Mitsubishi, you can get a single source hardware supply, engineering support and responsibility. Look for Mitsubishi, the world leader of gear manufacturing technology. For more information, call (312) 860-4220, NOW!

Heavy Duty Machine Tools | Machining Centers | FMS | Digitizer | CNC Lathes | Cylindrical Grinders | Special-Purpose Machine Tools | Gear Making Machine Tools | Precision Cutting Tools

MITSUBISHI HEAVY INDUSTRIES, LTD.
5-1, Marunouchi 2-chome, Chiyoda-ku, Tokyo, Japan
Cable Address: HISHIJU TOKYO

Mitsubishi Heavy Industries America, Inc.
873 Supreme Drive, Bensenville, IL 60160 Phone: (312) 860-4220

Mitsubishi International Corporation
873 Supreme Drive, Bensenville, IL 60160 Phone: (312) 860-4222

CIRCLE A-8 ON READER REPLY CARD

RANDALL PUBLISHING
1401 Lunt Avenue
P.O. Box 1426
Elk Grove, IL 60007
(312) 437-6604

The Advanced Technology of Leonardo Da Vinci 1452-1519

COVER

An illustration of what appears to be a single screw lifting device. Heavy objects were apparently attached to the hooks at the bottom of the screw. The crank-powered worm gear shown on the left would drive the screw and raise the objects off the ground. No further information is available about this particular sketch, one of hundreds of drawings of mechanical devices found in Leonardo's notebooks.

GEAR TECHNOLOGY

The Journal of Gear Manufacturing

CONTENTS — PAGE NO.

FEATURES

DEPARTMENTS

November/December, 1988 — Vol. 5, No. 6

GEAR TECHNOLOGY, The Journal of Gear Manufacturing (ISSN 0743-6858) is published bimonthly by Randall Publishing Co., Inc., 1425 Lunt Avenue, P. O. Box 1426, Elk Grove Village, IL 60007. GEAR TECHNOLOGY, The Journal of Gear Manufacturing. Subscription rates are: $40.00 in the United States, $50.00 in Canada, $55.00 in all other foreign countries. Second-Class postage paid at Arlington Heights, IL and at additional mailing office.

Postmaster: Send address changes to GEAR TECHNOLOGY, The Journal of Gear Manufacturing, 1425 Lunt Avenue, P. O. Box 1426, Elk Grove Village, IL 60007.

MANUSCRIPTS: We are requesting technical papers with an educational emphasis for anyone having anything to do with the design, manufacture, testing or processing of gears. Subjects sought are solutions to specific problems, explanations of new: technology, techniques, designs, processes, and alternative manufacturing methods. These can range from the "How to . . ." of gear cutting (BACK TO BASICS) to the most advanced technology. All manuscripts submitted will be carefully considered. However, the Publisher assumes no responsibility for the safety or return of manuscripts. Manuscripts must be accompanied by a self-addressed, self-stamped envelope, and be sent to GEAR TECHNOLOGY, The Journal of Gear Manufacturing, P.O. Box 1426, Elk Grove, IL 60009, (312) 437-6604.

EDITORIAL

MR. NONE-OF-THE-ABOVE WINS AGAIN

A few years ago, during a presidential election campaign, I saw an editorial cartoon that depicted a man standing outside a voting booth with a bemused expression on his face. Over the door to the booth was a quotation from Dante: "Abandon hope, all ye who enter here." Unfortunately for all of us, the grim jest is just as timely now. Once again, when we make our choice for president this year, the pick seems to be between Mr. Well-He's-Not-Actually-Awful and Mr. At-Least-He's-Not-The-Other-Guy. A candidate who can arouse truly positive and hopeful feelings in the electorate is once again not on the ballot.

Governor Dukakis bills himself as a new kind of Democrat—one who understands business, one who will be fiscally responsible, one who can produce a "miracle" for the country similar to the one he produced for Massachusetts. But a closer look reveals that the Massachusetts miracle may be as much blue smoke as economic recovery; and such recovery as has taken place has been financed by the largest tax increase in Massachusetts history. Having MIT and the hi-tech Mecca of Route 128 in Massachusetts didn't hurt any either.

Unfortunately, Mr. Dukakis' smug, puritanical moralizing, coupled with his ineffectual responses on some campaign issues, remind too many people of another governor with no experience in national government, Mr. Carter. I've been struck by the number of people from his own state and the rest of New England who speak with some skepticism about his attempts to shed this image and present the country with a "new" Michael Dukakis. The memories they have of the old one are not so pleasant, and they have doubts about how much of the "new" is real, and how much is convenient cosmetic change for the sake of the campaign.

The question on the minds of many people is, "Who really is Mike, and can he do any of the things he says he can?"

George Bush, Mr. Dukakis' Republican opponent, has his own problems with both his record and his image. He suffers from a bad case of foot-in-mouth disease and a tendency to lean too heavily on non-issues, like his opponent's opinion of the Pledge of Allegiance and his membership in the ACLU. There are many—some would say too many—unanswered questions about Mr. Bush's role in the Iran-Contra business and his switch from a critic of "voodoo economics" to a true believer in the Reagan brand of economic recovery financed by a huge national debt. His ability to choose advisors and team members who are not liabilities to him and at least some of his constituency is also open to question.

Perhaps more serious is a pervasive sense that we don't really know who Mr. Bush is either. A study of his record in government service shows us a possibly competent administrator and an expert at keeping a low profile. His performance has always been "adequate." Nothing awful has ever happened on his watch, but nothing outstandingly good either.

The answer to the Democrats' question, "Where was George?" seems to be, keeping his head down and staying out of trouble. That might be an admirable trait in a mid-level bureaucrat. It is not such a desirable position for the man who wants to be the leader of the free world. When sitting across the table from Mr. Gorbachev, arguably one of the most dynamic and brilliant Soviet leaders of the 20th century, Mr. Bush must be able to do better than "stay out of trouble."

This feeling of electoral malaise extends to the vice-presidential candidates as well. There may have been a time when we could say that the job didn't matter that much; that it was a ticket to four years of well-paid obscurity. Unfortunately, in a world increasingly dangerous and complex, being a heartbeat from the presidency is no casual matter. It *does* make a good deal of difference who holds that office—and neither of the vice-presidential candidates inspires the strong sense of security one would like to feel about the person who occupies it.

Lloyd Bentsen, Mr. Dukakis' running mate, is a tough, experienced Texas politician, but he is ideologically incompatible with the Massachusetts governor. One wonders if he could or would actually carry out Mr. Dukakis' programs if he had to assume the Presidency. Mr. Bentsen's personal and political finances also raise some troubling ethical questions. He is the owner of a legally required blind trust that watches his affairs with one eye open, and the inventor of the "Eggs McBentsen" breakfast, at which lobbyists, for a mere $10,000, could share toast and coffee with him. Do we wish

(continued on page 35)

GUEST EDITORIAL

AN INVITATION TO BE A CHAMPION

Recent history has taught us that global competition has become tougher and is a major concern of American gear manufacturers and users. The world has become smaller and manufacturers from abroad have invaded American markets with products designed in an environment where management of technology has been practiced effectively. If American companies intend to compete in the changing world market, they must acquire the technologies that will allow them to do so.

During the past several years, anti-trust laws have been liberalized to allow cooperation among competitors. Through a special type of cooperation, which the ASME Gear Research Institute has termed "Cooperative Pre-Competitive Research and Development," a better technology base can be established. Simply stated, Cooperative Pre-Competitive Research and Development is the pooling of resources and working together to create technologies without jeopardizing domestic competitive position.

The success of the concept has been proven throughout the world and, to a limited degree, in the United States. It has much to offer and is a good way to maximize return on dollars allocated to research.

The ASME Gear Research Institute is concerned with the relative lack of organized applied gear research being conducted in the United States when compared with that in Europe and Asia. Research programs in Europe are well organized and directed by members of the gear industry. The collected data is shared only by participants in the program. The work is sometimes made public, but not until several years after it has been completed; thus, offering the program participants adequate time to use the data to their competitive advantage.

Today some U.S. companies are working with European universities in developing gear technology. Apparently, they perceive that the European universities offer a service that no U.S. institution is capable of offering. This attitude is disturbing, since it indicates an apparent deficiency in the gear research conducted in the United States.

Gear manufacturers in the United States probably spend more total dollars for gear research than gear manufacturers of any country in the world, however, the work is done in corporate laboratories. The results are considered proprietary, and the work is usually fragmented, since it is done to satisfy a specific need of the corporation. Sometimes the same technology is being developed in several laboratories, each company spending its hard-earned research dollars to come to the same conclusions. It would be better for these companies to pool their resources and work together in these areas of common technology, developing more complete data that could be confidently used as a spring board for the proprietary research that leads to competitive advantage.

Daniel Boorstin, a noted historian and the Librarian of Congress from 1975 to 1987, tells us that every great discovery discloses unimagined realms of ignorance, and that the great obstacle to progress is not ignorance, but rather the illusion of knowledge. The courage to believe that we don't know what we think we know is the first step of discovery, and those who have this courage to believe are the prophets.

From my vantage point, I see several prophets who are becoming champions of gear research.

There is a champion from the worm gear industry who has begged for funds for a cooperative research program to better understand the operation of worm gears. With the help of ten interested companies, not all of whom are worm gear manufacturers, this champion has raised substantial funds for a three-year research project.

There are seven champions from the aerospace industry who have committed time, talent and funds for a five-year period to conduct gear research that they have defined as critical to their industry. They have already reached 70% of their goal, and have held two meetings of the steering committee to finalize their plans, and take the next step toward starting their research programs. There are seven more companies who are champions and have seen the need for cooperative gear research, pledging time, talent and funds for a five-year period to meet the technological needs of the gear industry.

These are the bright spots. However, there are still 120 gear manufacturers and users that must be convinced that to learn a technology, one must be a doer of research. It is good to update oneself by attending conferences, reading books and listening to speakers; however, remember that the information presented in those places *was* the state of the art three to four years ago.

The gear industry today has an opportunity to reshape U.S. gear research, to make it more meaningful, so that American geared products can again be competitive in the global marketplace. Why not be a part of this important activity by becoming a champion of U.S. gear research?

Donald L. Borden
V.P. Industrial Affairs
ASME-GRI

Donald L. Borden *is Vice President, Industrial Affairs, of ASME Gear Research Institute. He served as Vice President of the Technical Division of AGMA from 1976-1984 and is a member of the Technical Division Executive Committee. Currently, Mr. Borden is the conference chairman of the ASME 5th International Power Transmission and Gearing Conference.*

TECHNICAL CALENDAR

NOVEMBER 1-3. SME Gear Processing and Manufacturing Clinic, Sheraton Meridian, Indianapolis, IN. The technical conference will include papers on "Design and Selection of Hobs," "Selection of High-Speed Steel for Gear Cutting Tools," "Special Design Deburring Equipment" and other gear-related subjects. Attendees will have an opportunity to meet with presenters to discuss papers and ask questions on a one-on-one basis. Tuesday evening will feature a reception and tabletop exhibits from major manufacturers. For further information, call Dominic Ahearn at SME Headquarters, (313) 271-1500 x384.

NOVEMBER 5-10. International Conference on Gearing, Zhengzhou, China. ASME-GRI and several international gear organizations are sponsoring this meeting. For more information contact: Inter-Gear '88 Secretariat, Zhengzhou Research Institute of Mechanical Engineering, Zhongyuan Rd, Zhengzhou, Henan, China. Tel: 47102. Cable 3000. Telex 46033 HSTEC CN.

NOVEMBER 8-10. American Society for Metals Near Net Shape Manufacturing Conference, Hyatt Regency, Columbus, OH. Program will cover precision casting, powder metallurgy, design of dies and molds, forging technology and inspection of precision parts. For further information contact: Technical Department Marketing, ASM International, Metals Park, OH 44073.

NOV. 30-DEC. 2. Gear Seminar, Milwaukee, WI. The Center for Continuing Engineering, University of Wisconsin-Milwaukee, is offering a three-day seminar on "Fundamentals of Gear Design." It will cover the basic design considerations in the development of properly functioning gear systems. The course is aimed at the designer, user and beginning gear technologist. For more information, contact: John Leaman, Center for Continuing Engineering Ed., UW-M, 929 North Sixth St., Milwaukee, WI 53203. (414) 227-3110.

APRIL 25-27, 1989. ASME 5th Annual Power Transmission & Gearing Conference, Chicago, IL. Presentations on emerging technologies for gears, couplings and other power transmission devices, gear geometry, noise, manufacturing and other gear-related subjects. For more information, contact Donald Borden, P.O. Box 502, Elm Grove, WI 53122.

AGMA TECHNICAL EDUCATION SEMINARS. AGMA is offering a new series of technical education seminars, each one focusing on a different aspect of gear manufacturing and taught by industry experts.

Nov. 9, Cincinnati, OH. "Controlling the Carburizing Process."

Dec. 7, AGMA Headquarters, Alexandria, VA. "Rational Loose Gear Quality Requirements for the Specifier and Purchaser. (Using The Gear Standard AGMA 2000 Properly.)"

Jan. 11, Cincinnati, OH. "Specifying and Controlling the Quality of Shot Peening."

March 7/8, Rochester, NY. "Source Inspection of Loose Gears from the Customer's Standpoint."

May 2, Cincinnati, OH. "Gear Math at the Shop Level for the Gear Shop Foreman."

June 6, AGMA Headquarters. "Specifying and Verifying Material Quality per AGMA Material Grades."

For more information, contact: Bill Daniels, AGMA, 1500 King St., Suite 201, Alexandria, VA 22314. (703) 684-0211.

VIEWPOINT

Letters for this column should be addressed to Letters to the Editor, GEAR TECHNOLOGY, P.O. Box 1426, Elk Grove Village, IL 60009. Letters submitted to this column become the property of GEAR TECHNOLOGY. Names will be withheld upon request; however, no anonymous letters will be published. Opinions expressed by contributors are not necessarily those of the editor or publishing staff.

Dear Editor:

I was particularly happy to have Bill Janninck's article on worm gear contact ("Contact Surface Topology of Worm Gear Teeth," Mar/Apr. 1988) as we have had many an exchange on this over the years.

I would like to point out that material on Wire Measurements of Helical Gears and Worms is found on pp 40-42 of my *Revised Manual of Gear Design*. The calculation of MOWs for helical gears is not immediately obvious from the spur gear calculations, and while it is covered in Earle Buckingham's *Analytical Mechanics of Gears* in inverse form, I receive many calls from engineers wanting to know how to do this particular calculation.

The wire measurement on worms is generally not known. The most common method is to use the Vogel equations, which were designed for screw threads, and are very complex and cumbersome. The equations treating the worm as an involute helecoid are much simpler, apply regardless of the form on the worm and are also applicable to any type of VEE screw thread. If a wire is selected to contact the pitch point, the result will be the same as the Vogel equations. If the exact wire is not used, as one is rarely going to make a special gage wire, using the involute equations are MORE accurate than the Vogel method using the approximations for compensating for the wrong wire. The only place I know of these equations being published before is in an article of mine on "Worm and Spur Gear Drives" which came out in *Machine Design*, March 3, 1966.

Eliot K. Buckingham
President,
Buckingham Associates, Inc.

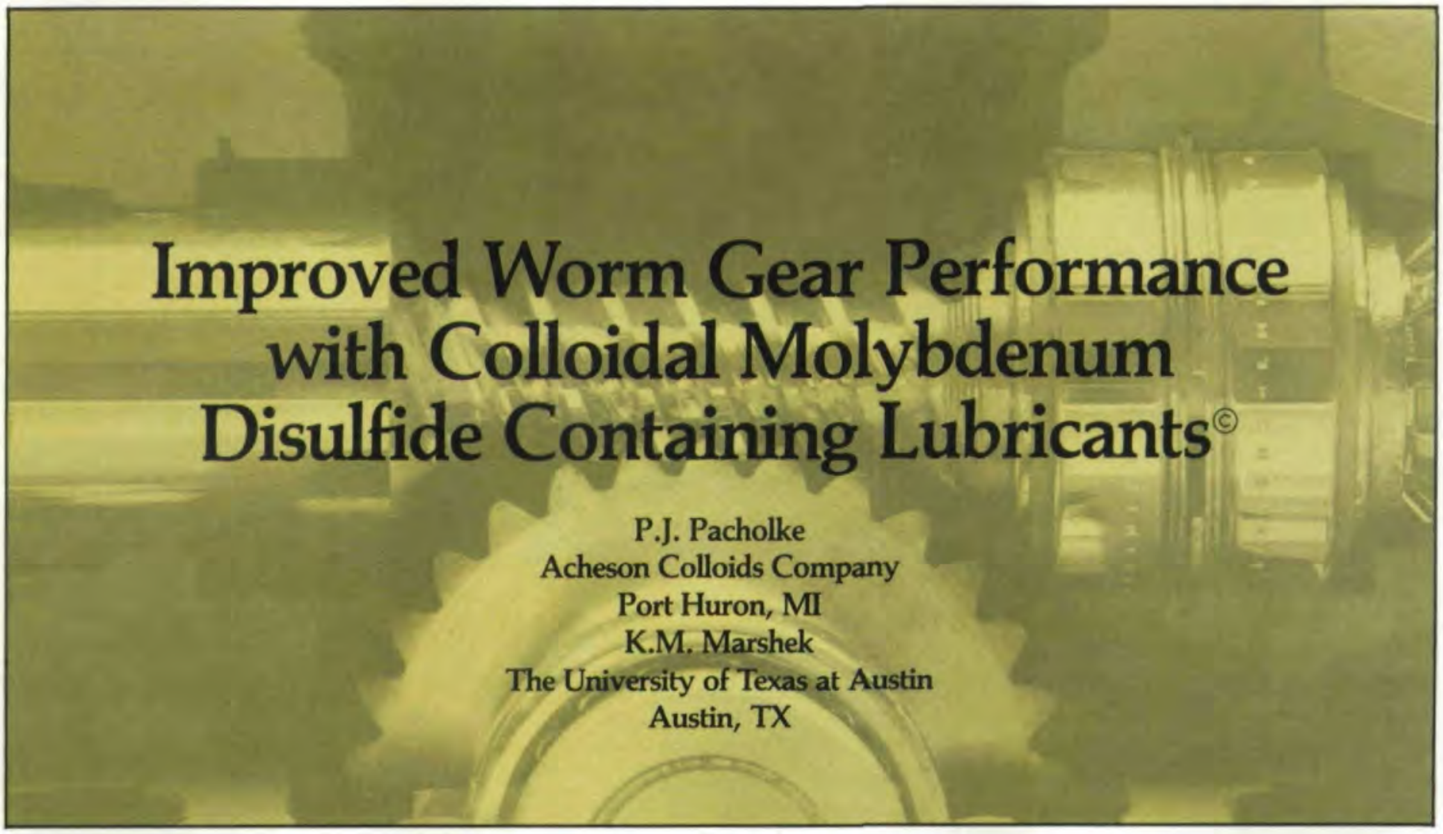

Improved Worm Gear Performance with Colloidal Molybdenum Disulfide Containing Lubricants©

P.J. Pacholke
Acheson Colloids Company
Port Huron, MI
K.M. Marshek
The University of Texas at Austin
Austin, TX

Abstract:

Worm gear speed reducers give the design engineer considerable options, but these gear systems present a challenge to the lubrication engineer. Heat energy generated by the high rate of sliding and friction in the contact zone causes worm gears to be relatively inefficient compared to other gear types. Because worm gears operate under a boundary or near-boundary lubrication regime, a satisfactory lubricant should contain a friction modifier to alleviate these conditions.

Experimental results show that the addition of speciallly formulated colloidal molybdenum disulfide containing additives to gear lubricants can increase efficiency, lower operating temperatures through sliding friction reduction and reduce gear wear and break-in time.

Introduction

Compactness, dependability, a wide selection of reduction ratios in a single unit, and lower cost compared to other speed reducers make worm gear drives a good design choice. The inefficiency of worm gear reducers has been ignored in recent years as the energy crisis of the early 1970s gave way to a relative abundance of fuel today.

Industry analysts have projected an annual energy cost savings of six billion dollars if worm gear lubricants contained just 1.0% colloidal MoS_2.[1] These calculations were based on the assumption that there are an estimated three million worm gear speed reducers rated at an average of 10 hp currently in service in the United States. If the efficiency of these units was increased by 5% (for example, from 68.8% to 72.2%) with 1.0% stable colloidal MoS_2, the energy savings would amount to 98 billion kW-h, which, at \$0.06/kW-h, amount to six billion dollars. These data, based on AGMA (American Gear Manufacturers Association) estimates, do not even include the several million more worm gear reducers which are rated at less than 5 hp.

Even though energy conservation may not be receiving as much attention and priority today, the bottom-line savings that lubricants containing stable colloidal molybdenum disulfide can offer should not be ignored by a world faced with a finite energy supply.

The very design of worm gearing results in a high rate of sliding which generates a great deal of heat energy. There is a con-

AUTHORS:

PAULA J. PACHOLKE *is the staff research chemist in charge of lubricant and lubricant additive research at Acheson Colloids Company, a division of Acheson Industries, Inc. She holds a Bachelor of Science in Chemistry from Alma College, Alma, MI, and has done graduate work at the Saginaw Valley State University. Ms. Pacholke is the Chairman of the Solid Lubricants technical section of the Industrial Lubricants Subcommittee of ASTM. She is also a member of the Society of Tribologists and Lubrication Engineers, SAE and the American Chemical Society. She holds a US patent for a demulsible solid lubricant oil additive and lubricant which has the unique ability to remove emulsified water without the necessity of demulsifying chemicals.*

DR. KURT M. MARSHEK, *is Professor of Mechanical Engineering and Gulf Oil Fellow at The University of Texas at Austin. He is a registered professional engineer in Texas and Ohio and has written more than 120 papers and technical reports. He holds four patents in the area of mechanical design and analysis. In 1973, Dr. Marshek was awarded the SAE Ralph R. Teetor Award for his contributions to research, teaching and student development; in 1980, he was named an Outstanding Teacher, Cullen College of Engineering at the University of Houston; in 1985, he received the University of Texas at Austin, College of Engineering, Faculty Leadership Award and the Halliburton Education Foundation Award of Excellence, in recognition of outstanding achievement and professionalism in education, research and service to students.*

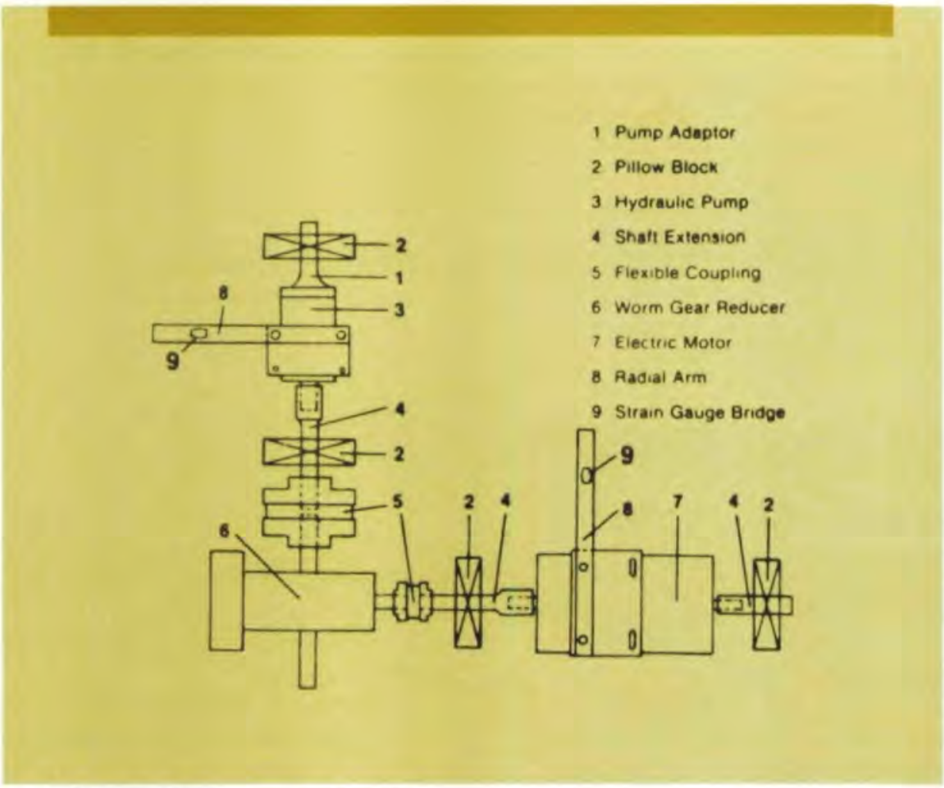

Fig. 1—Worm gear dynamometer test machine.

siderable loss of output power, primarily as thermal energy. (About 75% of the output power lost by worm gearing can be attributed to the generation of thermal energy by sliding friction. Minor power losses are due to churning, bearing friction and other miscellaneous causes.) Output power generated by worm gear reducers operating at high speeds, loads and reduction ratios is consequently limited by thermal constraints rather than mechanical limits.[2] Higher oil temperatures result in shortened lubricant life, and worm gear reducers often require external cooling to reduce oil temperatures to an acceptable level.

Worm gear efficiency is defined as the ratio of output power to input power and depends indirectly on speed-reducer reduction ratios. Efficiency in worm gear reducers ranges from 50-90%, compared to hypoid and similar gearing, which are 85-97% efficient. The relative inefficiency in worm gears is a result of the sliding friction created between the contacting surfaces of the worm and the driven gear, whereas, in spur and helical gearing, the contact between mating surfaces is predominately rolling. For low reduction ratios, worm gearing is between 70% and 90% efficient, but a high reduction ratio of 60:1 would have a rated efficiency of only about 50%.[3] In the higher reduction ratios, therefore, even a small percentage increase in efficiency would translate into fairly substantial energy savings.

Lubricants designed for worm gear reducers should perform two major functions:

1. Reduce friction and wear to improve efficiency and extend gear life.
2. Act as a heat transfer medium to conduct heat energy away from the contact zone.

Worm gears operate predominantly under boundary lubrication conditions. Hydrodynamic or thick film lubrication does not exist because of the high rate of sliding, high contact pressures and tooth geometry found in worm gears. Boundary lubrication conditions require the use of specialized additives which can provide the lubrication necessary to prevent metal-to-metal contact in the absence of a thick oil film.

The traditional worm gear lubricant is a high-viscosity oil compounded with "oiliness" or lubricity components, such as acidless tallow or synthesized fatty esters. These compounded oils function to relieve boundary lubrication conditions by providing an adsorbed layer of molecules which easily shear on the contacting surfaces of the gear teeth. Acidless tallow added to the oil reduces operating temperatures to acceptable levels, but the efficiency of the reducer is not significantly affected.

Studies have shown that dispersed solid lubricants, such as molybdenum disulfide or graphite, increase efficiency and, hence, reduce energy consumption in automotive engines and gearing.[3, 4, 5] Initial work by Smith and Marshek indicated that the use of 1.0% by weight of stable colloidal MoS_2 in worm gear lubricants improved efficiency and reduced oil temperatures in the baseline fluid studied. This work showed that oils blended with MoS_2 in stable colloidal form significantly improved worm gear performance, whereas, earlier studies had not detected this effect because the molybdenum disulfide powder was merely stirred into the test oil, where it immediately settled and was not available as a boundary friction modifier. With stable colloidal MoS_2, however, the molybdenum disulfide is available throughout the entire recommended oil change period and does not settle out in properly formulated lubricants.

Maintenance engineers have long expressed a desire for a more universal oil, one which would function in all types of gear systems and which would also provide the specialized lubrication required in worm gearing. The present study examined the concept of a "universal" gear oil, a lower viscosity base oil which would contain a specially designed package of stable, dispersed MoS_2 and oxidation inhibitors, and which would properly lubricate both worm gear speed reducers and other gear types.

Apparatus and Procedure

A worm gear dynamometer test machine was used to evaluate the various performance aspects of the worm gear speed reducer (Fig. 1). A 30:1 reduction ratio, fan-cooled unit was powered by a 1.5 hp, 1720 rpm, ac motor. The load on the reducer was supplied by a hydraulic gear pump circulating automatic transmission fluid through a closed loop. The fluid was circulated through a water-cooled heat exchanger to maintain a fluid temperature less than 56°C.

Both the motor and gear pump were supported by their shafts in pillow blocks to allow freedom of rotation. Connections between the system components were made with flexible couplings to minimize any effects of misalignment. A radial arm was bolted to the gear pump housing so that torque could be transmitted from the housing to the radial arm which provided the load on the worm gear reducer. The load was controlled by adjusting the back pressure in the gear pump hydraulic loop with a pressure control valve.

Output torque was measured by a strain gauge mounted on the radial arm in a full-bridge configuration. Input torque was measured in a similar way.

Thermal measurements were made by T-type (copper-constantan) thermocouples placed in the reducer sump, the hydraulic fluid reserve tank and in the ambient air.

All measurement transducers on the worm gear dynamometer were monitored by a data acquisition system controlled by a microcomputer. Interface cards accepted wiring from strain gauges and thermocouples for direct input into the acquisition system. Measured values were converted directly into engineering units by utilizing the microcomputer software. Output data were stored on floppy disk and hard copy provided by printer and plotter.

Test Parameters. Output torque was maintained at 113 N·m (1000 in·lbf), allowing input torque to vary as a function of lubricant performance. The ambient temperature was controlled at 25°C in an air-conditioned laboratory. Fan cooling was provided to keep the oil in the reducer sump below 95°C.

Break-in Test Procedure. This portion of the study was designed to characterize and compare the break-in of two identical worm gear sets using two lubricants — the factory-fill AGMA No. 8 compounded and AGMA No. 7 (uncompounded) containing 1.0% colloidal MoS_2 (by weight) as a specially formulated, stable additive package.

A new steel worm and bronze gear set was installed and properly aligned in the reducer for each test. One-half liter of test lubricant was prepared and placed in the reducer. All test parameters — input and output torque together with reducer oil sump, gear pump transmission fluid and ambient air temperatures — were monitored by the data acquisition system.

1. The reducer was run at 56.5 N·m (50 in·lbf), approximately half its rated output torque, until a steady-state temperature of <95°C was attained.
2. Output load was incrementally increased to a final output torque of 113 N·m (1000 in·lbf). The reducer was required to achieve steady-state operation; i.e., reducer oil sump temperature <95°C) before the load was increased to the next level.
3. Once the steady-state operation at 113 N·m output torque was attained, efficiency calculations were made.
4. Upon completing the prescribed break-in procedures, the test lubricant was removed from the reducer and the unit thoroughly flushed with solvent.

Performance Testing. Efficiency and other performance parameters of candidate worm gear lubricants were measured on a gear set installed in the worm gear test dynamometer and run in with AGMA No. 8 compounded oil to steady-state operating conditions. Output torque was held constant at 113 N·m, and oil sump temperatures were required to be less than 95°C whenever possible.

1. The test lubricant was prepared as necessary. For tests with lubricants containing MoS_2, specially formulated dispersion packages were blended into the lubricant prior to filling the reducer sump.
2. One-half liter of test lubricant was added to the reducer sump, and the reducer was started with no applied output load.
3. The back pressure control valve on the gear pump reserve fluid tank was slowly closed to bring the output torque to the 113 N·m test load.
4. The reducer was allowed to achieve steady-state operation. (Steady-state operation in this study is defined as: output torque = 113 N·m and reducer oil sump temperature constant and <95°C.) Once the unit had reached the steady-state condition, the load on the strain gauges was removed and unstrained readings taken for both strain gauge bridges.
5. Output torque was returned to 113 N·m and the steady-state conditions.
6. Monitoring of the test parameters was initiated by the data acquisition unit and continued throughout the two-hour test period. One hundred measurements from each transducer were averaged every 146 seconds during the test.
7. The microcomputer then calculated and printed a table of the mean values and standard deviations of the test parameters.
8. The test lubricant was drained from the reducer and sump. The unit was then double-flushed with a volatile solvent to minimize any possible carry-over effects from individual lubricants. This process was considered sufficient to remove mechanically occluded MoS_2 contained in conventional mineral-oil-based lubricants as determined by previous work.

Test Lubricants. The test lubricants and molybdenum disulfide dispersion packages evaluated in this study are described in Tables 1 and 2, respectively. The selected lubricants were chosen to represent:

1. A typical factory-fill worm gear oil – AGMA No. 8 compounded
2. AGMA No. 8 compounded with 1.0% colloidal MoS_2 (by weight)
3. A lower viscosity oil – uncompounded AGMA No. 7 with 1.0% colloidal MoS_2 as a boundary friction modifier
4. Two synthetic lubricants – polyalphaolefin and polyalkylene glycol.

Results and Discussion

Break-in Studies. AGMA No. 7 (uncompounded) gear oil containing 1.0% colloidal MoS_2 substantially reduced the time necessary to achieve steady-state operating conditions in the worm gear test apparatus, when compared to the same procedure carried out using the manufacturer's recommended AGMA No. 8 compounded oil. This reduction is clearly shown in Fig. 2. Accompanying the reduced time to

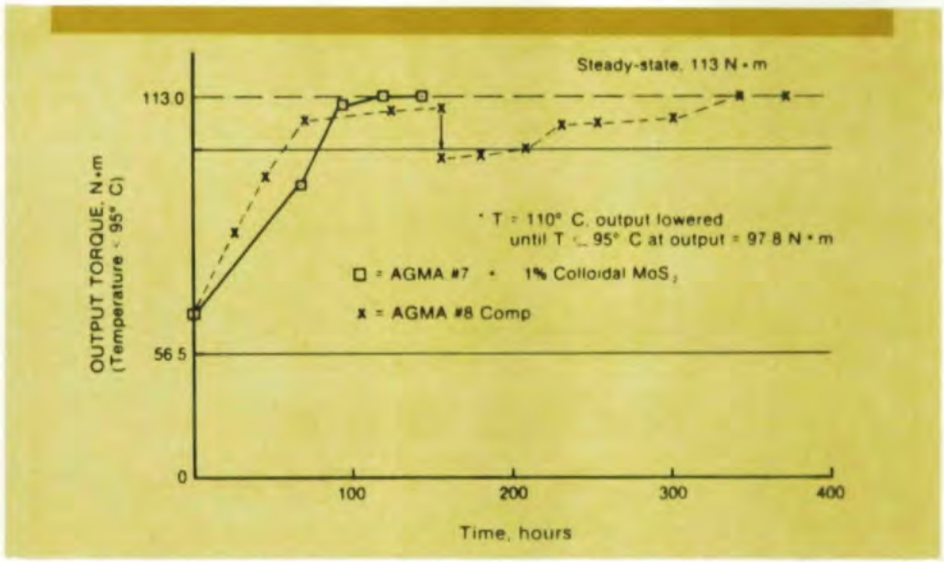

Fig. 2 – Comparison of time to achieve steady-state operation (output torque = 113 N·m, oil sump temperature <95°C).

TABLE 1—DESCRIPTION OF WORM GEAR TEST LUBRICANTS

Fluid ID	Description	Kinematic Viscosity, cSt		Viscosity* Index
		40°C	100°C	
A	AGMA No. 8 Comp	631.7	32.75	80
B	AGMA No. 8 Comp + 1.0% Colloidal MoS_2 as Dispersion Package 1	642.9	33.75	84
C	AGMA No. 7 + 1.0% Colloidal MoS_2 as Dispersion Package 1	466.6	29.97	92
D	AGMA No. 7	458.5	29.50	92
E	AGMA No. 7 + Additive Package 2 (Package 1 without MoS_2)	433.5	28.40	92
F	Synthetic No. 1, Polyalphaolefin	62.38	10.25	134
G	Synthetic No. 1 + 1.0% Colloidal MoS_2 as Dispersion Package 3	66.24	9.975	125
H	Synthetic No. 2, Polyalkylene Glycol	59.56	10.92	145
I	Synthetic No. 2 + 1.0% Colloidal MoS_2 as Dispersion Package 4	61.68	10.34	136

*Calculated as per ASTM D-2270

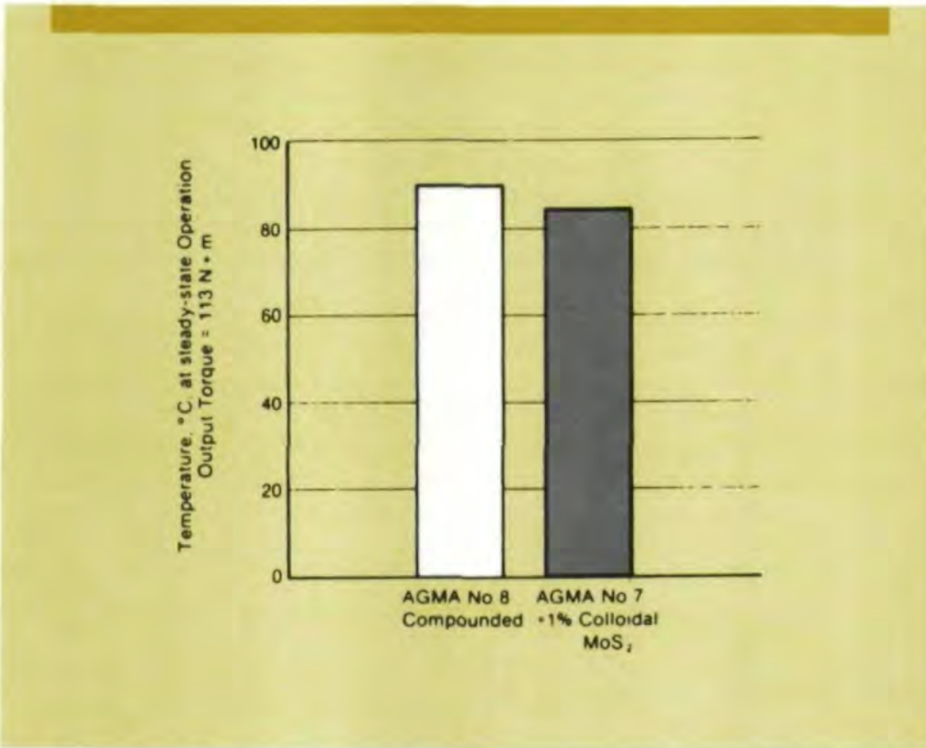

Fig. 3 – Comparison of oil sump temperature at steady-state operation: AGMA No. 7 + 1.0% colloidal MoS_2 vs AGMA No. 8 compounded.

reach operating conditions of 113 N·m and oil temperatures less than 95°C with the use of the MoS_2-containing AGMA No. 7, was a significant reduction in oil sump temperatures at a constant level of output torque. Fig. 3 compares the temperatures of the two break-in test oils at steady-state operation.

Performance Evaluations. The performance criteria of interest were input torque and calculated efficiency as an indication of the energy expenditure effects of each lubricant. Oil sump temperatures were examined as an indication of the heat transfer ability of the lubricant. The addition of stable dispersed molybdenum disulfide to test lubricants lowered the input torque needed to drive the worm gear test reducer at a standard output torque of 113 N·m. Table 3 describes the performance characteristics of all the fluids: mean input torque, efficiency and oil sump temperatures. The most dramatic increase in efficiency and decreased operating oil sump temperatures in a test lubricant formulated with 1.0% colloidal MoS_2 by weight was exhibited by the synthetic lubricants – Fluids F, G, H and I. Fig. 4 compares the efficiencies of test lubricants with and without 1.0% stable colloidal MoS_2.

Efficiency Studies. Test lubricant F, the the polyalphaolefin without MoS_2, had an efficiency similar to that of Fluid B (AGMA No. 8 compounded plus 1.0% coloidal MoS_2). The addition of 1.0% MoS_2 as a PAO-based additive package (Fluid G) increased the efficiency of this PAO lubricant from 63.2% to 67.8%, a 7.3% increase in efficiency.

Synthetic No. 2, the polyalkylene glycol Fluid H, ran less efficiently than any lubricant tested. However, the addition of MoS_2 in a polyalkylene glycol-based dispersion package improved efficiency by 5.3% – from 61.8% to 65.1% efficiency.

Fluids D and E were control lubricants used to examine any possible effect soluble components of the dispersion additive packages might have on worm gear performance. Neither lubricant D nor E gave the same level of efficiency or the reduced input torque exhibited by Fluid C (AGMA No. 7 base oil with 1.0% colloidal MoS_2). Both Fluid D and Fluid E performed comparably to Fluid A, the factory-fill AGMA No. 8 compounded gear oil. These test results indicate that a lower viscosity oil, blended with a stable MoS_2 additive package, provides the necessary friction modification to improve power transmission efficiency by reducing sliding friction. Fluid C (No. 7 plus 1.0% colloidal MoS_2) had a mean efficiency of 64.0%, whereas, the conventionally compounded No. 8 oil (Fluid A) operated at a mean efficiency of only 62.6%. This improvement translates to a 2.2% increase in efficiency.

Statistical analysis showed that the probability that these differences in performance are real exceeds 99.99%.

Temperature Effects. No statistically signficant variations in oil temperatures were observed in the group of high-viscosity AGMA No. 7 (uncompounded) and No. 8 (compounded) fluids. This apparent lack of differentiation between oils containing dispersed MoS_2 and untreated oils is most likely due to the heat energy generated by the excessive churning of the lubricant and the generally poor heat transfer capabilities of high-viscosity fluids. The lone exception to this generality is Fluid E, which had been tested after the synthetic plus MoS_2 Fluid G. Despite stringent measures to eliminate carryover between test fluids, the baseline oil, run just before and after the PAO series of fluids, indicated a consistent and significant decrease in oil tempertures (<90°C) similar to those developed by Fluid B during the last one hour of its test period. The esta-

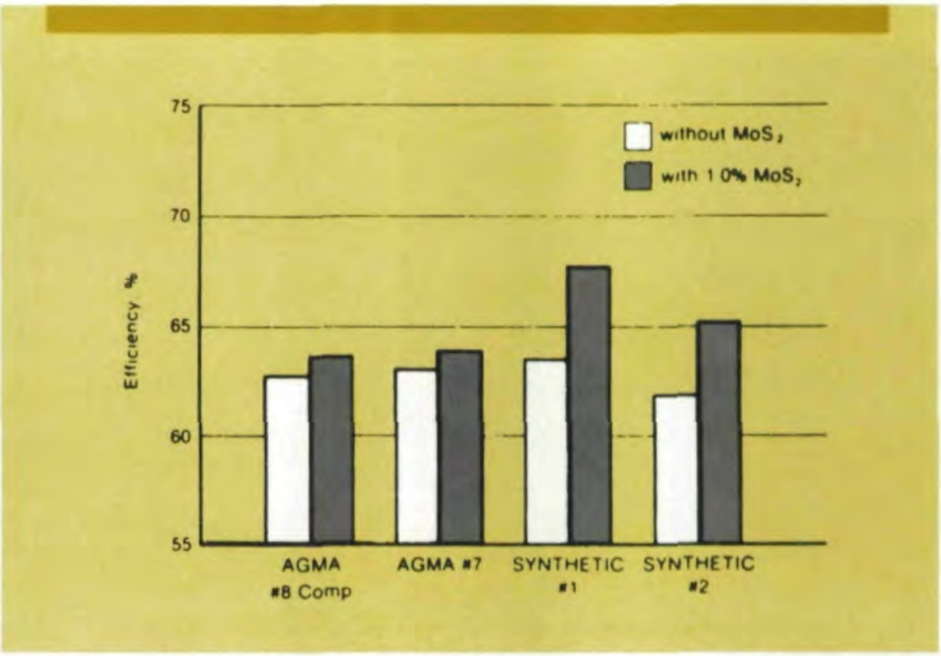

Fig. 4 – Efficiency comparison of test lubricants with and without 1.0% stable colloidal MoS_2.

Table 2—Description of Stable Colloidal MoS_2 Additive Packages	
Dispersion Package	Description
1	MoS_2 Dispersed in 150 Solvent Neutral Oil
2	Package 1 without MoS_2
3	MoS_2 Dispersed in Polyalphaolefin
4	MoS_2 Dispersed in Polyalkylene Glycol

Table 3—Results of Worm Gear Dynamometer Tests					
		Performance Parameters Output Torque = 113 N·m			
Fluid ID	Description	Mean Input Torque, N·m	Std. Dev.	Percent Efficiency	Mean Oil Sump Temperature, °C
A	AGMA No. 8 Comp	6.02	0.054	62.6	92.1
B	AGMA No. 8 Comp + 1.0% Colloidal MoS_2 Dispersion Additive 1	5.92	0.107	63.6	95.5
C	AGMA No. 7 + 1% MoS_2 as Dispersion Additive 1	5.89	0.079	64.0	93.4
D	AGMA No. 7	6.05	0.075	62.3	93.6
E	AGMA No. 7 + Additive 2 (Additive 1 Package without MoS_2)	5.99	0.080	62.9	86.5*
F	Synthetic No. 1, Polyalphaolefin	5.96	0.110	63.2	97.5
G	Synthetic No. 1 + 1% Colloidal MoS_2 as Dispersion Additive 3	5.56	0.017	67.8	91.0
H	Synthetic No. 2, Polyalkylene Glycol	6.09	0.080	61.8	108.8
I	Synthetic No. 2 + 1% Colloidal MoS_2 as Dispersion Additive 4	5.79	0.117	65.1	88.4

*Lower temperature attributed to minor Fluid G carry-over. See text.

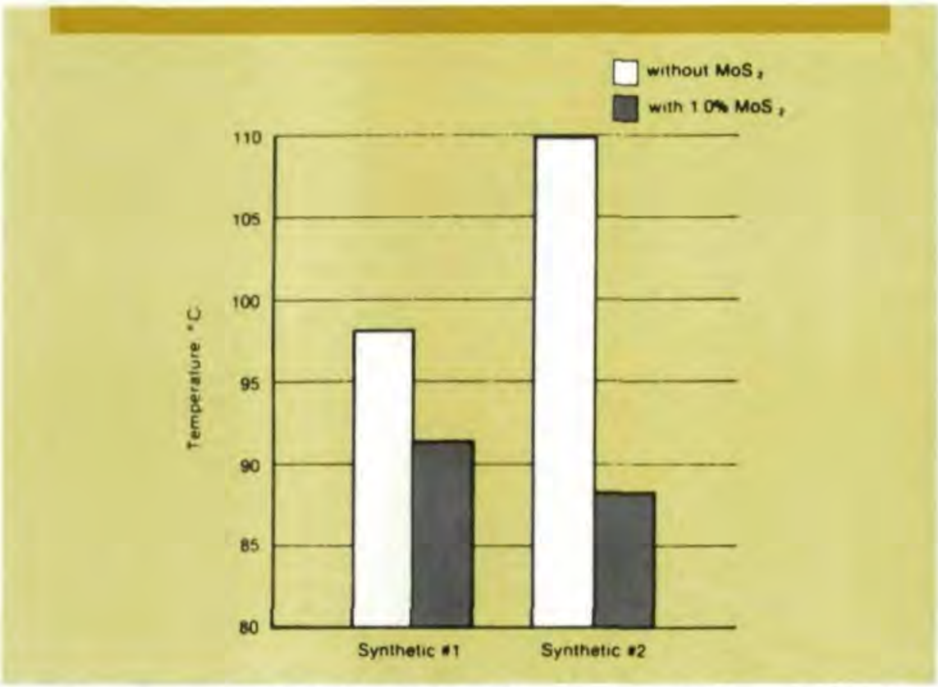

Fig. 5 — Temperature-reduction effects of the addition of 1.0% stable, dispersed MoS_2 to synthetic lubricants 1 and 2.

blished input torque baseline data allowed the calculation of an appropriate input torque correction factor to be applied to the input torque values of Fluid E.

The temperature reduction benefits of 1.0% colloidal molybdenum disulfide in lubricants are clearly observed in the two synthetic fluids. Both Synthetic No. 1 and Synthetic No. 2 are considerably lower in viscosity (Table 1) than any of Fluids A – E. Although the synthetic fluids have higher viscosity indexes compared to most petroleum-based oils, they do not always provide adequate boundary friction lubrication. In the PAO series, Fluids F and G, the addition of 1.0% stable, dispersed MoS_2 reduced the mean operating oil temperature by 6.5°C: from 97.5°C for Fluid F to 91.0°C for Fluid G as shown in Fig. 5. It should also be noted that the oil sump temperatures for Fluid G were substantially lower during the last hour of the efficiency test.

An even greater decrease in mean oil sump temperatures was observed with the polyalkylene glycols. Fig. 5 shows that the addition of 1.0% colloidal MoS_2 resulted in a 20.4°C decrease in mean oil sump temperatures. Fluid H had a mean temperature of 108.8°C, whereas Fluid I, which contained MoS_2, had a mean temperature of 88.4°C. There is a probability that the decreases in oil sump temperatures observed with the synthetic lubricants containing colloidal MoS_2 are real exceed 99.99%.

Conclusions

This study showed that the addition of 1.0% molybdenum disulfide (as a stable, colloidal dispersion package) to an AGMA No. 7 gear oil reduced the time required to break in a gear set to an output power equivalent to the factory-fill AGMA No. 8 compounded oil by 60.2%: 139 hours for the AGMA No. 7 plus colloidal MoS_2 to reach an output of 113 N·m, compared to the 349 hours required for the AGMA No. 8 compounded to reach the same conditions. A significant reduction in the final steady-state operating temperature was also observed: 90°C for the AGMA No. 8 compounded versus 84.4°C for the AGMA No. 7 plus 1.0% colloidal MoS_2.

The addition of colloidal MoS_2 to worm gear lubricants also significantly increased power transmission efficiency by reducing sliding friction and allowing the reducer to operate at the same level of output power for a smaller expenditure of input power. This decreased input power requirement appeared to be the case for conventional oils containing MoS_2, as well as with similarly treated synthetic lubricants. There is greater than a 99.9% certainty that these improvements are real.

The treatment of high-viscosity oils with 1.0% colloidal MoS_2 (AGMA No. 8 compounded and AGMA No. 7) did not appear to have a measureable effect on oil temperatures because of the poor heat energy transfer properties of such oils. However, lower viscosity fluids of high-viscosity index, such as the synthetic polyalphaolefins and polyalkylene glycols, when blended with 1.0% colloidal MoS_2, exhibited real and significant reductions of operating oil tempertures.

It can then be reasonably presumed that 1.0% colloidal molybdenum disulfide can increase the performance in worm gear speed reducers with considerable cost savings in energy consumption, and can also reduce operating temperatures in certain lubricants and extend lubricant life by reducing the rate of oil oxidation. Only the lubricants containing stable colloidal MoS_2 offered these performance benefits. In such stable lubricant systems, the molybdenum disulfide particles remain in suspension throughout the normal lubricant lifespan, whereas, noncolloidal MoS_2, simply stirred into lubricants, flocculates and settles almost immediately to the bottom of the gear box and is not available as a solid lubricant friction modifier. All these parameters of worm gear performance can be correlated to reduced friction due to the improved boundary lubrication conditions resulting in less wear, quieter operation and longer lubricant and gear box life.

References

1. MISKA, KURT H., Ed. "MoS_2 Addition Boosts Efficiency in Worm Gear Speed Reducers," *Molydisulfide Newsletter*, XXVII, 1, AMAX Metals Group, Ann Arbor, MI, January, 1985.
2. Anonymous. *The Speed Reducer Book*, Winsmith Div. VMC Industries, Inc., Springville, NY, pp 67-69, 1980.
3. SMITH, R.K. and MARSHEK, K.M. "Lubricants Containing Dispersed Molybdenum Disulfide Improve Worm Gear Efficiency," *NLGI Spokesman*, XLVIII, 2, pp 47-54, May, 1984.
4. GRESTY, D.A., KUNZ, E.J., Jr., RISDON, T.J. "The Effect of MoS_2 Based Lubricants on Automotive Gear Efficiency and Operating Temperatures," SAE 770834, Soc. of Automotive Engs., Inc., Warrendale, PA, 1977.
5. BENNINGTON, J.E., et al. "Stable Colloid Additives for Engine Oils – Potential Improvements in Fuel Economy," SAE 750677, Soc. of Automotive Engs., Inc. Warrendale, PA, 1975.

Acknowledgement:

Reprinted courtesy of the Society of Tribologists and Lubrication Engineers. Presented at 41st Annual Meeting, Toronto, Canada, May 12-15, 1986.

Gear Tooth Profile Determination From Arbitrary Rack Geometry

Sandeep M. Vijayakar,
Biplab Sarkar,
Donald R. Houser,
The Ohio State University, Columbus, Ohio

Abstract:

This article describes a method of obtaining gear tooth profiles from the geometry of the rack (or hob) that is used to generate the gear. This method works for arbitrary rack geometries, including the case when only a numerical description of the rack is available. Examples of a simple rack, rack with protuberances and a hob with root chamfer are described. The application of this technique to the generation of boundary element meshes for gear tooth strength calculation and the generation of finite element models for the frictional contact analysis of gear pairs is also described.

Introduction

After selection of the basic gear tooth geometry, the proper design of the tooth profile is probably the next most important factor in successful gear design. Aspects of proper gear design, such as the minimization of the transmission error to reduce noise, load sharing between teeth, the strength of the teeth and the stresses in the fillet all depend upon the tooth profile and root geometry. Procedures that compute the transmission error need an accurate numercial description of the gear tooth profile, as do gear tooth strength calculating methods, such as boundary element and finite element methods, which need accurate load sharing information and rely heavily on the accuracy of the tooth profile itself. They also need accurate numercial descriptions of the gear tooth fillet. An approximate fillet description, such as a circular arc of an approximately

AUTHORS:

DR. SANDEEP M. VIJAYAKAR *received his BTech degree from the Indian Institute of Technology at Bombay and his M.S. and Ph.D. from Ohio State University. He is currently a research associate at Ohio State and a member of ASME.*

DR. DONALD R. HOUSER *is on the faculty of the Department of Mechanical Engineering, Ohio State University. In addition to his teaching responsibilities, he has researched and published in the areas of gear dynamics and noise, v-belts, vibration diagnostics and vibration signal analysis. He is also currently director of the university's Gear Dynamics and Gear Noise Research Laboratory. Dr. Houser is a member of ASME, SAE, AGMA and Tau Beta Pi, Pi Tau Sigma and Sigma Xi honorary fraternities. He is also chairman of the ASME Power Transmission and Gearing Committee. Dr. Houser received his degrees in Mechanical Engineering from the University of Wisconsin at Madison.*

BIPLAB SARKAR *received his Bachelor of Technology in mechanical engineering in 1985 from the Indian Institute of Technology, Kharagpur, India, and his Master of Science degree in 1988 from The Ohio State University. He is currently working on a doctorate in mechanical engineering at The Ohio State University. His areas of interest include gear manufacture and measurement and CAD/CAM.*

computed radius, is not adequate for this purpose.

When a gear is generated by a rack (which includes a hob) with straight sides and circular corners, the tooth profile is an involute with trochoids at the fillets. The equations for such a gear can be obtained in analytical form, such as in the text by Colbourne.[1] In practice, however, various modifications, such as protuberances and profile modifications, may be applied to the rack. The corner of the hob itself need not be circular, and there may be a chamfer of specified dimensions. In such cases, it is not always possible to come up with an analytical form for the gear tooth profile.

Chang et al.[2] described a methodology to generate the involute profile on a computer from a straight sided rack. Hefeng et al.[3] described a technique that would also generate the trochoidal portion of the gear tooth profile which is generated by the circular corners at the tip of the rack. In the technique described in that article, for every relative orientation of the gear with respect to the rack, a point on the gear was found at which the normal passed through the pitch point, thus generating the profile. This technique, however, required an analytical description of the rack tooth profile. When the rack tooth profile is defined numerically or when the rack profile is more complicated than a set of straight lines and circles, the method was found to be difficult to use.

In this article, a method is described which is general enough to numerically compute the gear tooth profile of a generated gear tooth, given the geometry of the rack. Instead of searching along the rack profile to find a point which satisfies the meshing condition for a fixed relative orientation, this method determines the relative orientation of the gear and the rack for which a fixed point on the rack satisfies the condition of meshing. This method is more amenable to dealing with complicated rack profiles for which closed form equations are either not available or are too cumbersome to work with. It can also take into account the undercutting in gears. Even though it is not presented here, the method is also applicable to shaper cut geometries.

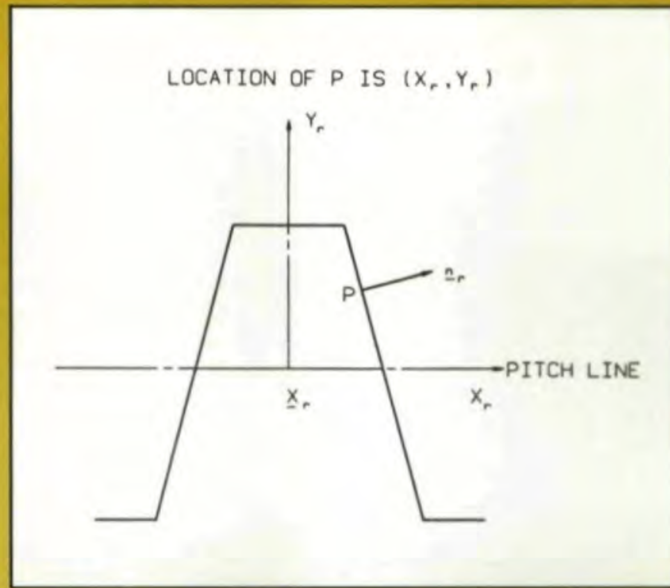

Fig. 1 – The rack and its attached coordinate system.

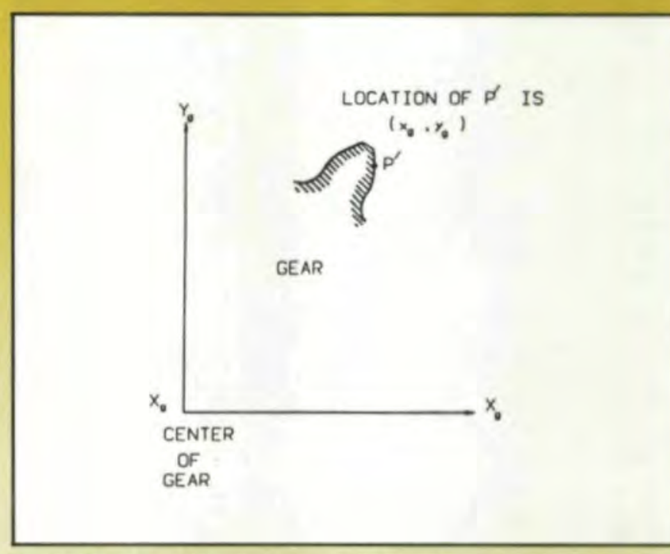

Fig. 2 – The gear and its attached coordinate system.

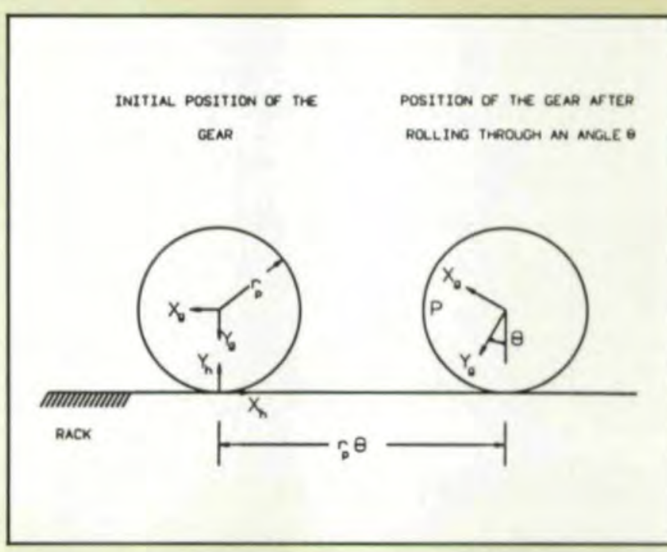

Fig. 3 – The relative orientation of the gear and rack coordinates systems during generation.

Profile Generation Algorithm

The input data required for this algorithm consist of a description of the rack that generates the gear, the number of teeth on the gear and the outer diameter of the gear. Fig. 1 shows a coordinate system $\underline{X}_r$ attached to a rack. The origin of this coordinate system lies on the pitch line of the rack. Let $\underline{x}_r = (x_r, y_r)$ be the coordinates of an arbitrary point P on the rack profile, with respect to the coordinate system $\underline{X}_r$ attached to the rack. Let $\underline{n}_r = (n_x, n_y)$ be the outward unit normal to the rack at this point. For any specified rack geometry, the coordinates and the normal vector at any point on the rack profile are easily obtained.

Fig. 2 shows a gear tooth with an attached coordinate system $\underline{X}_g$ with its origin at the center of the gear. Let P' be a point on the gear tooth profile that corresponds to the point P on the rack. In other words, as the gear rolls through with the rack, the point P on the rack makes sliding contact with the point P' on the gear. Let $\underline{x}_g = (x_g, y_g)$ be the coordinates of the point P' on the gear with respect to the coordinate system $\underline{X}_g$ attached to the gear.

This algorithm uses the coordinate and unit normal vector data available for the point P to compute the coordinates of the point P'. Fig. 3 shows the relative position of the gear and rack

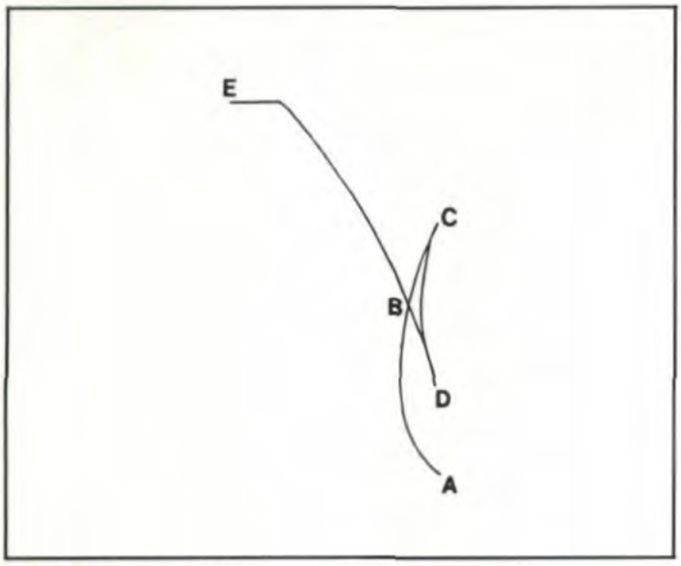

Fig. 4 – Gear tooth profile generated when undercutting occurs.

at a starting position and at a position after the gear has rolled through an angle θ. The pitch circle radius of the gear is r. For this arbitrary orientation of the gear, the transformation from the rack coordinate system to the gear coordinate system is defined by the matrix equation:

$$\begin{Bmatrix} x_g \\ y_g \end{Bmatrix} = \begin{bmatrix} -\cos\theta & \sin\theta \\ -\sin\theta & -\cos\theta \end{bmatrix} \begin{Bmatrix} x_r - r\theta \\ y_r - r \end{Bmatrix} \qquad (1)$$

As the gear rolls, the relative velocity of the point P′ on the gear with respect to the rack is

$$\underline{v} = \begin{Bmatrix} r\dot{\theta} \\ 0 \end{Bmatrix} + \dot{\theta} \begin{Bmatrix} y_r - r \\ r\theta - x_r \end{Bmatrix}$$

the first part being the translational contribution, and the second part being the rotational contribution. $\dot{\theta}$ is the time derivative of θ. Hence,

$$\underline{v} = \dot{\theta} \begin{Bmatrix} y_r \\ r\theta - x_r \end{Bmatrix}$$

According to the equation of meshing, this relative velocity of the point on the gear should have no component normal to the rack, such that the dot product

$$\underline{v} \cdot \begin{Bmatrix} n_x \\ n_y \end{Bmatrix} = 0$$

or,

$$y_r n_x + (r\theta - x_r)\, n_y = 0$$

Thus the roll angle at which the point P makes contact with a point on the gear is given by

$$\theta = \frac{x_r n_y - y_r n_x}{r n_y} \qquad (2)$$

Given any point P on the rack, its coordinates and its normal vector, the roll angle at which it makes contact with the gear can be computed from Equation 2. The coordinates of the corresponding point P on the gear can then be obtained by substituting for θ in Equation 1. Therefore, a sequence of points on the gear tooth profile can be found that correspond to a sequence of points on the rack profile.

The next step is to examine the gear tooth profile thus obtained for possible undercutting. If undercutting does take place, the gear tooth profile will look like Fig. 4. The part B-C-D-B has to be detected, and the points in this part have to be eliminated from the sequence of points that define the profile of the gear tooth.

Let $\{\underline{r}_i;\ i=1,n\}$ be a sequence of coordinates corresponding to the points on the gear tooth profile. To detect the cross-over point B shown in Fig. 4, we need to check whether there exist integers i and j such that the line segment (i,i+1), which joins $\underline{r}_i$ with point $\underline{r}_{i+1}$ intersects the line segment (j−1, j). Fig. 5 shows two line segments, (a,b) and (c,d). These line segments will in-

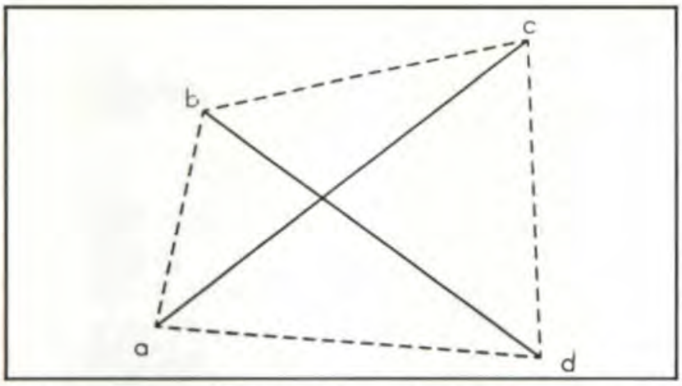

Fig. 5 – Determination of the point of intersection of two line segments.

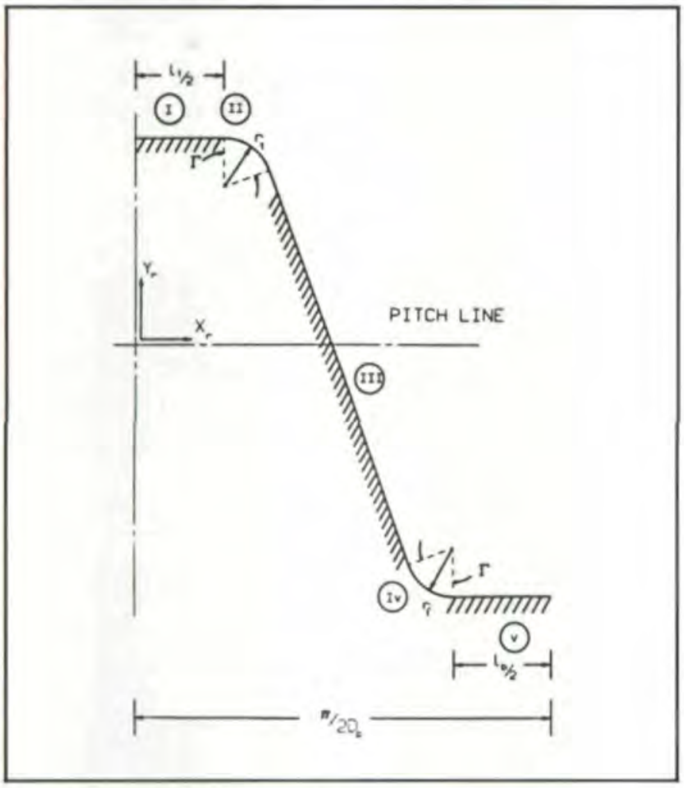

Fig. 6 – Geometry of an elementary rack.

tersect if and only if

$$A(a,b,c) \cdot A(a,b,d) < 0$$

and

$$A(c,d,a) \cdot A(c,d,b) < 0$$

where

$$A(a,b,c) = (\underline{r}_b - \underline{r}_a) \times (\underline{r}_c - \underline{r}_a)$$

where $\underline{r}_a$, $\underline{r}_b$, and $\underline{r}_c$ are three-dimensional coordinates of the three points a, b and c, respectively; the "x" stands for a vector cross product and the · stands for the vector inner product.

$$\underline{r}_a = \begin{Bmatrix} x_a \\ y_a \\ 0 \end{Bmatrix}, \ \underline{r}_b = \begin{Bmatrix} x_b \\ y_b \\ 0 \end{Bmatrix} \text{ and}$$

$$\underline{r}_c = \begin{Bmatrix} x_c \\ y_c \\ 0 \end{Bmatrix}$$

The location of the point of intersection $\underline{r}_e$ will be

$$\underline{r}_e = \alpha\, \underline{r}_a + (1 - \alpha)\underline{r}_b$$

where $$\alpha = \frac{\| A(c,d,b,) \|}{\| A(c,d,a) \| + \| A(c,d,b) \|}$$

Using this method, the whole profile can be searched for segments $(i, i+1)$ and $(j-1, j)$ that intersect. If such an i and j are found, then all points on the profile between $i+1$ and $j-1$ are discarded and replaced by a single point, the point of intersection.

A similar condition occurs at the tip of the gear tooth when the radius at the root of the rack profile is not large enough, or when there is a chamfer at the root of the rack profile. The same technique can be used to eliminate points that cannot possibly lie on the gear tooth.

Geometry of a Simple Rack. Fig. 6 shows a simple rack.

Let D_p = Diametral pitch,
A = Addendum,
B = Dedendum,
ϕ = Pressure angle,
r_t = Radius at tip of rack tooth,
r_f = Radius at fillet of rack tooth,

$$\Gamma = \frac{\pi}{2} - \phi$$

$$l_t = \frac{\pi}{2D_p} - 2A \tan(\phi) - 2r_t \tan\left(\frac{\Gamma}{2}\right)$$

$$l_b = \frac{\pi}{2D_p} - 2B \tan(\phi) - 2r_f \tan\left(\frac{\Gamma}{2}\right)$$

Coordinates of points along the rack profile are then given by:

In region I (the top land),

$$\begin{Bmatrix} x_r \\ y_r \end{Bmatrix} = \begin{Bmatrix} \beta l_t/2 \\ A \end{Bmatrix}$$

$$\begin{Bmatrix} n_x \\ n_y \end{Bmatrix} = \begin{Bmatrix} 0 \\ 1 \end{Bmatrix} \quad 0 < \beta \leq 1$$

In region II (the tip radius),

$$\begin{Bmatrix} x_r \\ y_r \end{Bmatrix} = \begin{Bmatrix} l_t/2 + r_t \sin(\beta\Gamma] \\ A - r_t(1 - \cos(\beta\Gamma)) \end{Bmatrix}$$

$$\begin{Bmatrix} n_x \\ n_y \end{Bmatrix} = \begin{Bmatrix} \mathrm{Sin}(\beta\Gamma) \\ \mathrm{Cos}\,(\beta\Gamma) \end{Bmatrix} \quad 0 < \beta \leq 1$$

In region III (the tooth flank),

$$\begin{Bmatrix} x_r \\ y_r \end{Bmatrix} = (1-\beta) \begin{Bmatrix} l_t/2 + r_t \sin\Gamma \\ A - r_t(1 - \cos\Gamma) \end{Bmatrix}$$

$$+ \beta \begin{Bmatrix} \pi/2D_p - l_b/2 - r_f \mathrm{Sin}\Gamma \\ -B + r_f(1\text{-}\cos\Gamma) \end{Bmatrix}$$

$$\begin{Bmatrix} n_x \\ n_y \end{Bmatrix} = \begin{Bmatrix} \text{Cos}\phi \\ \text{Sin}\phi \end{Bmatrix} \quad 0 < \beta \leq 1$$

In region IV (the root fillet),

$$\begin{Bmatrix} x_r \\ y_r \end{Bmatrix} = \begin{Bmatrix} \pi/2D_p - l_b/2 - r_f\text{Sin}((1-\beta)\Gamma) \\ -B + r_f(1-\cos((1-\beta)\Gamma) \end{Bmatrix}$$

$$\begin{Bmatrix} n_x \\ n_y \end{Bmatrix} = \begin{Bmatrix} \text{Sin}((1-\beta)\Gamma) \\ \text{Cos}((1-\beta)\Gamma) \end{Bmatrix} \quad 0 < \beta \leq 1$$

In region V (the bottom land),

$$\begin{Bmatrix} x_r \\ y_r \end{Bmatrix} = \begin{Bmatrix} \pi/2D_p - (l_b/2)(1-\beta) \\ -B \end{Bmatrix}$$

$$\begin{Bmatrix} n_x \\ n_y \end{Bmatrix} = \begin{Bmatrix} 0 \\ 1 \end{Bmatrix} \quad 0 < \beta \leq 1$$

Geometry of a Rack with Protuberance. Fig. 7 shows a rack with protuberance.

Let α = Protuberance angle,
d = Protuberance high point distance,
l = Parallel land length,

$$l_t = \frac{\pi}{2D_p} - 2A\tan(\phi) - 2r_t\tan(\frac{\Gamma}{2}) + 2(\frac{d}{\cos\phi})$$

$$l_b = \frac{\pi}{2\,D_p} - 2B\tan(\phi) - 2r_f\tan(\frac{\Gamma}{2})$$

Coordinates of points along the profile of the rack with protuberance are then given by:

In region I (the top land),

$$\begin{Bmatrix} x_r \\ y_r \end{Bmatrix} = \begin{Bmatrix} \beta l_t/2 \\ A \end{Bmatrix}$$

$$\begin{Bmatrix} n_x \\ n_y \end{Bmatrix} = \begin{Bmatrix} 0 \\ 1 \end{Bmatrix} \quad 0 < \beta \leq 1$$

In region II (the tip radius),

$$\begin{Bmatrix} x_r \\ y_r \end{Bmatrix} = \begin{Bmatrix} l_t/2 + r_t\sin(\beta\Gamma) \\ A - r_t(1-\cos(\beta\Gamma)) \end{Bmatrix}$$

$$\begin{Bmatrix} n_x \\ n_y \end{Bmatrix} = \begin{Bmatrix} \text{Sin}(\beta\Gamma) \\ \text{Cos}(\beta\Gamma) \end{Bmatrix} \quad 0 < \beta \leq 1$$

In region III (the parallel land),

$$\begin{Bmatrix} x_r \\ y_r \end{Bmatrix} = \begin{Bmatrix} l_t/2 + r_t\sin\Gamma + \beta l\sin\phi \\ A - r_t(1-\cos\Gamma) - \beta l\cos\phi \end{Bmatrix}$$

$$\begin{Bmatrix} n_x \\ n_y \end{Bmatrix} = \begin{Bmatrix} \cos\phi \\ \sin\phi \end{Bmatrix} \quad 0 < \beta \leq 1$$

In region IV (protuberance angle length),

$$\begin{Bmatrix} x_r \\ y_r \end{Bmatrix} = \begin{Bmatrix} l_t/2 + r_t\sin\Gamma + l\sin\phi \\ A - r_t(1-\cos\Gamma) - l\cos\phi \end{Bmatrix} + \beta \begin{Bmatrix} (d/\sin\alpha)\sin(\phi-\alpha) \\ -(d/\sin\alpha)\cos(\phi-\alpha) \end{Bmatrix}$$

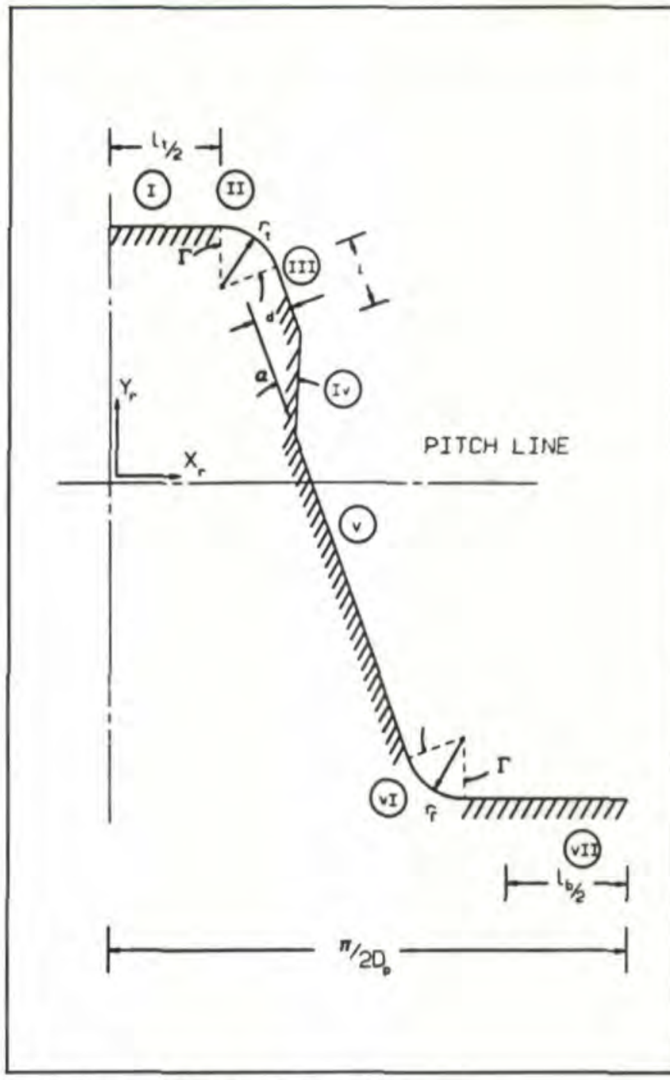

Fig. 7 – Geometry of a rack with a protuberance.

$$\begin{Bmatrix} n_x \\ n_y \end{Bmatrix} = \begin{Bmatrix} \cos(\phi-\alpha) \\ \sin(\phi-\alpha) \end{Bmatrix} \quad 0 < \beta \leq 1$$

In region V (the tooth flank),

$$\begin{Bmatrix} x_r \\ y_r \end{Bmatrix} = (1-\beta) \begin{Bmatrix} l_t/2 + r_t\sin\Gamma + l\sin\phi \\ A - r_t(1-\cos\Gamma) - l\cos\phi \end{Bmatrix} + (1-\beta)(d/\sin\alpha) \begin{Bmatrix} \sin(\phi-\alpha) \\ -\cos(\phi-\alpha) \end{Bmatrix} + \beta \begin{Bmatrix} \pi/2D_p - l_b/2 - r_f\text{Sin}\Gamma \\ -B + r_f(1-\cos\Gamma) \end{Bmatrix}$$

$$\begin{Bmatrix} n_x \\ n_y \end{Bmatrix} = \begin{Bmatrix} \cos\phi \\ \sin\phi \end{Bmatrix} \quad 0 < \beta \leq 1$$

In region VI (the root fillet),

$$\begin{Bmatrix} x_r \\ y_r \end{Bmatrix} =$$

$$\begin{Bmatrix} \pi/2D_p - l_b/2 - r_f \mathrm{Sin}((1-\beta)\Gamma) \\ -B + r_f(1-\cos((1-\beta)\Gamma) \end{Bmatrix}$$

$$\begin{Bmatrix} n_x \\ n_y \end{Bmatrix} = \begin{Bmatrix} \mathrm{Sin}((1-\beta)\Gamma) \\ \mathrm{Cos}((1-\beta)\Gamma) \end{Bmatrix} \quad 0 < \beta \leq 1$$

In region VII (the bottom land),

$$\begin{Bmatrix} x_r \\ y_r \end{Bmatrix} = \begin{Bmatrix} \pi/2D_p - (l_b/2)(1-\beta) \\ -B \end{Bmatrix}$$

$$\begin{Bmatrix} n_x \\ n_y \end{Bmatrix} = \begin{Bmatrix} 0 \\ 1 \end{Bmatrix} \quad 0 < \beta \leq 1$$

Geometry of a Hob with Root Chamfer. Often hobs with root chamfers are used to provide tip relief on the gear. Fig. 8 shows such a hob with a chamfer. Then

$$l_t = \frac{\pi}{2D_p} - 2A\tan(\phi) - 2r_t\tan(\frac{\Gamma}{2})$$

$$l_b = \frac{\pi}{2D_p} - 2B\tan(\phi)$$

$$- 2L_1(\tan\eta - \tan\phi)$$

where $\eta = \tan^{-1}(L_2/L_1)$

where L_1 and L_2 define the root chamfer as shown in Fig. 8. Coordinates of points along the rack profile are then given by:

In region I (the top land),

$$\begin{Bmatrix} x_r \\ y_r \end{Bmatrix} = \begin{Bmatrix} \beta l_t/2 \\ A \end{Bmatrix}$$

$$\begin{Bmatrix} n_y \\ n_y \end{Bmatrix} = \begin{Bmatrix} 0 \\ 1 \end{Bmatrix} = 0 < \beta \leq 1$$

In region II (the tip radius),

$$\begin{Bmatrix} x_r \\ y_r \end{Bmatrix} = \begin{Bmatrix} l_t/2 + r_t\sin(\beta\Gamma) \\ A - r_t(1-\cos(\beta\Gamma)) \end{Bmatrix}$$

$$\begin{Bmatrix} n_x \\ n_y \end{Bmatrix} = \begin{Bmatrix} \mathrm{Sin}\,(\beta\Gamma) \\ \mathrm{Cos}\,(\beta\Gamma) \end{Bmatrix} \quad 0 < \beta \leq 1$$

In region III (the tooth flank),

$$\begin{Bmatrix} x_r \\ y_r \end{Bmatrix} = (1-\beta) \begin{Bmatrix} l_t/2 + r_t\sin\Gamma \\ A - r_t(1-\cos\Gamma) \end{Bmatrix}$$

$$+ \beta \begin{Bmatrix} \pi/2D_p - l_b/2 - L_2 \\ -B + L_1 \end{Bmatrix}$$

$$\begin{Bmatrix} n_x \\ n_y \end{Bmatrix} = \begin{Bmatrix} \mathrm{Cos}\phi \\ \mathrm{Sin}\phi \end{Bmatrix} \quad 0 < \beta \leq 1$$

In region IV (the root chamfer),

$$\begin{Bmatrix} x_r \\ y_r \end{Bmatrix} \begin{Bmatrix} \pi/2D_p - l_b/2 - L_2(1-\beta) \\ -B + L_1(1-\beta) \end{Bmatrix}$$

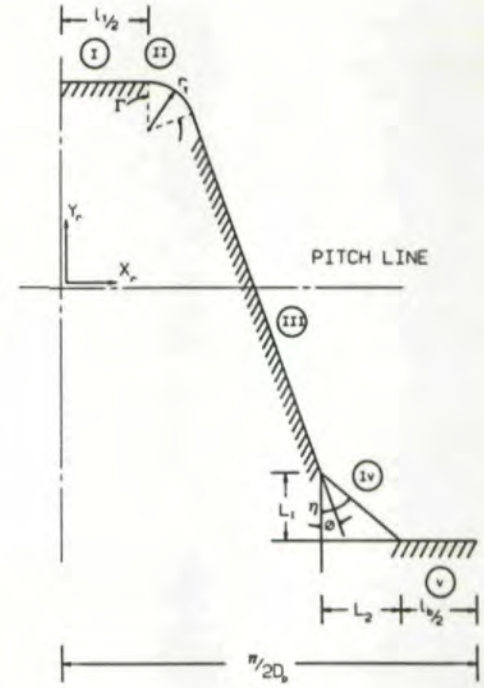

Fig. 8 – Geometry of a hob with root chamfer.

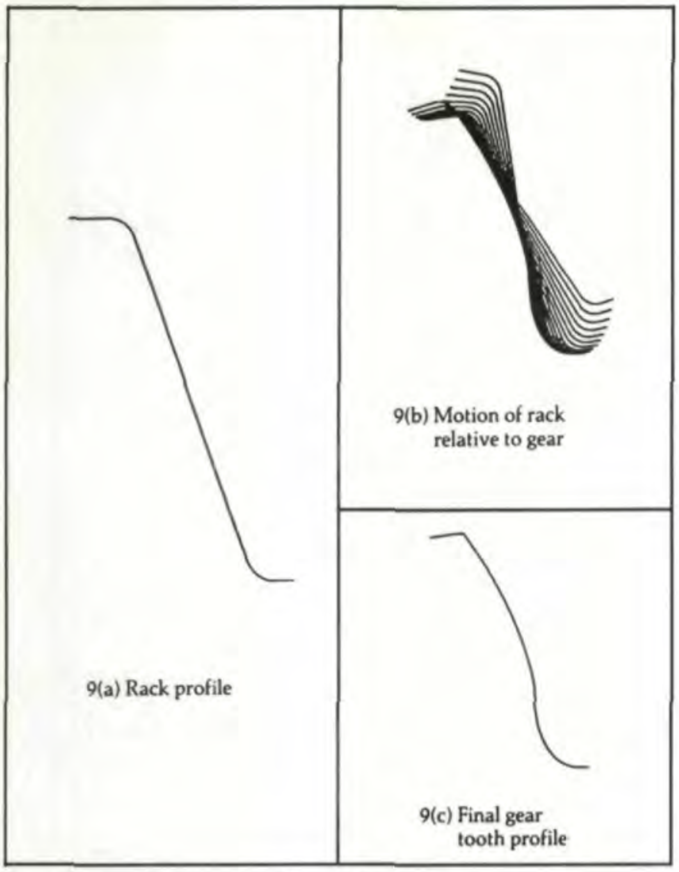

Fig. 9 – Generation of a gear with a simple rack.

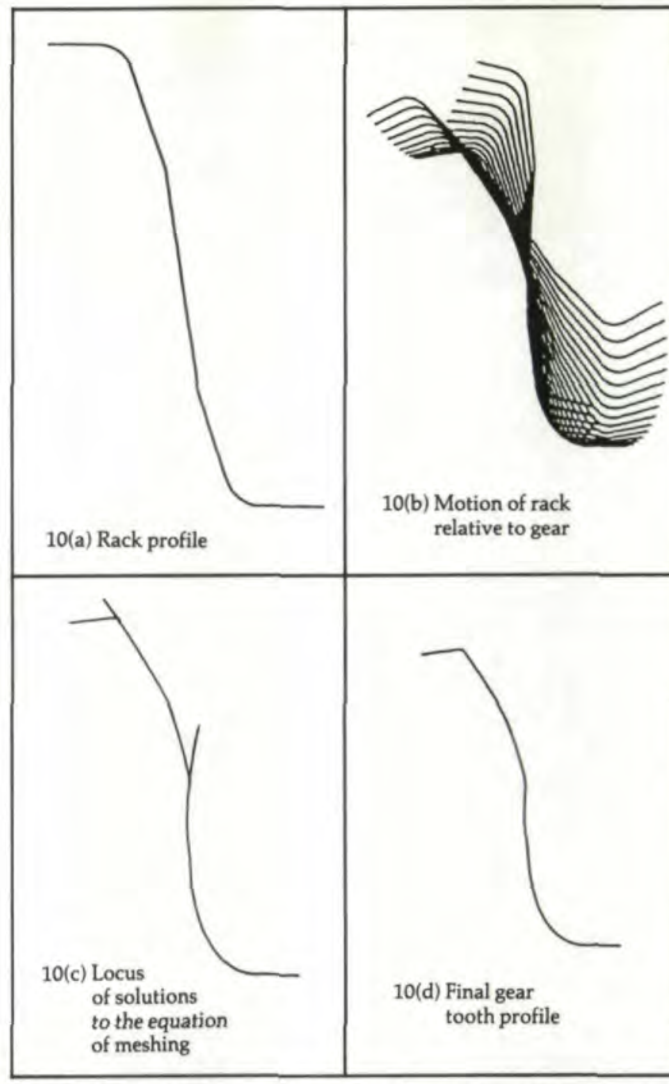

Fig. 10 – Generation of a gear using a rack with a protuberance angle $\alpha = 10°$.

$$\begin{Bmatrix} n_x \\ n_y \end{Bmatrix} = \begin{Bmatrix} \text{Cos}\eta \\ \text{Sin}\eta \end{Bmatrix} \; 0 < \beta \leq 1$$

In region V (the bottom land),

$$\begin{Bmatrix} x_r \\ y_r \end{Bmatrix} = \begin{Bmatrix} \pi/2D_p - (l_b/2)(1-\beta) \\ -B \end{Bmatrix}$$

$$\begin{Bmatrix} n_x \\ n_y \end{Bmatrix} = \begin{Bmatrix} 0 \\ 1 \end{Bmatrix} \; 0 < \beta \leq 1$$

Profile Generation Examples. Consider a basic rack with pressure angle $\phi = 20°$, with a diametral pitch $D_p = 10$ per inch, an addendum constant of 1.4, dedendum constant of 1.0 and a tip radius $r_t = 0.02''$.

Fig. 9(a) shows such a rack with no protuberance and with a root fillet radius $r_f = 0.02$ inches. Fig. 9(b) shows the positions of the rack relative to the generated gear as a gear with 20 teeth rolls through. Fig. 9(c) shows the gear tooth profile, which is obtained by using the procedure described earlier.

Fig. 10(a) shows the same rack, but with a protuberance angle $\alpha = 10°$, a parallel land length $l = 0.05$ inches and protuberance high point distance $d = 0.02$ inches. Fig. 10(b) shows the motion of the rack relative to the gear and Fig. 10(c) shows

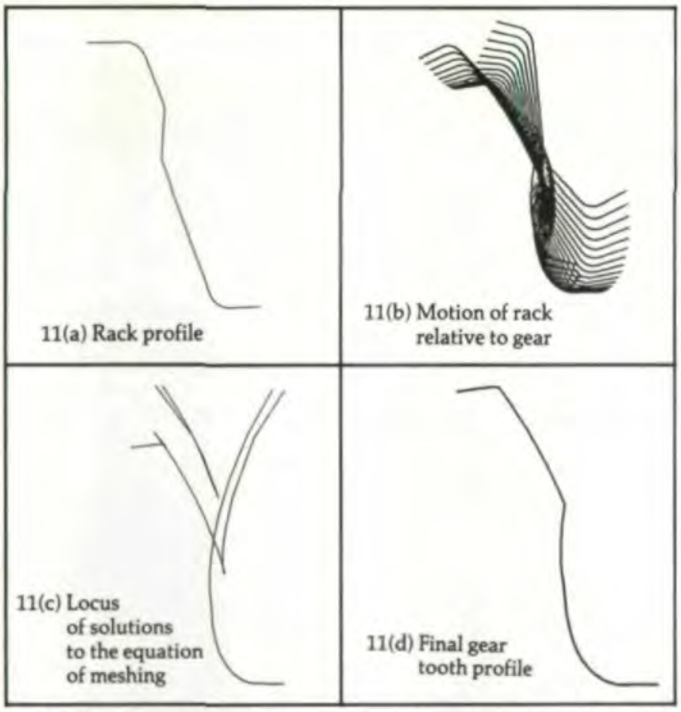

Fig. 11 – Generation of a gear using a rack with a protuberance angle $\alpha = 25°$.

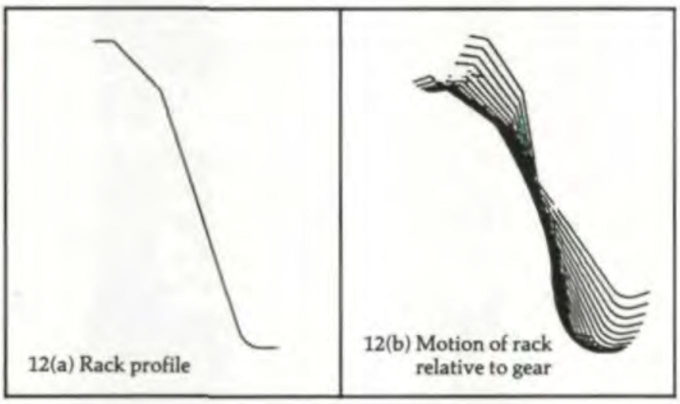

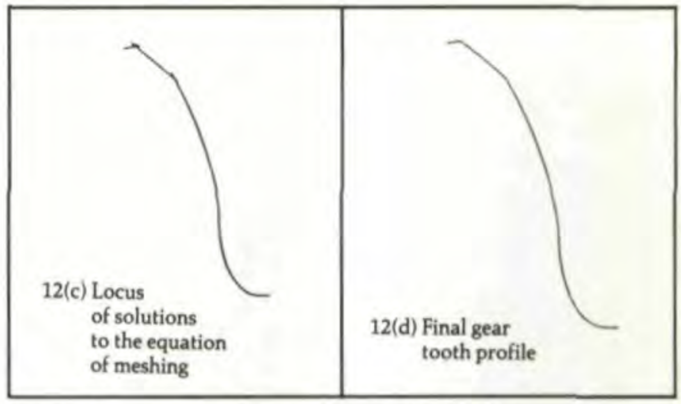

Fig. 12 – Generation of a gear using a rack with a chamfer.

the locus of the points that are solutions to the equation of meshing. Note the severe undercutting and the presence of non-feasible points at the gear tooth tip and at the intersection of the involute section of the gear tooth profile with the trochoidal root. Fig. 10(d) shows the final profile, obtained after all non-feasible points have been eliminated using the procedure described earlier in this paper. Figs. 11(a) through (d) show the same process for an extremely exaggerated case with protuberance angle $\alpha = 25°$.

Figs. 12(a) through (d) show a similar hob with a root chamfer with intercepts $L_1 = 0.04''$ and $L_2 = 0.04''$. (See Fig. 8.)

In order to keep to the more practical rack geometries, the examples described here had rack profiles which were made up of straight lines and circles, but the method may be applied to arbitrary geometries with equal ease.

Applications.

a) In Computer-Aided Design Programs: The simplest use to which this procedure can be put is that of drawing gears for different rack geometries as part of general computer-aided design programs. It can show the severity of undercutting and allow the designer through the use of zoom features to accurately predict the shape of the tooth which is being developed. Fig. 13

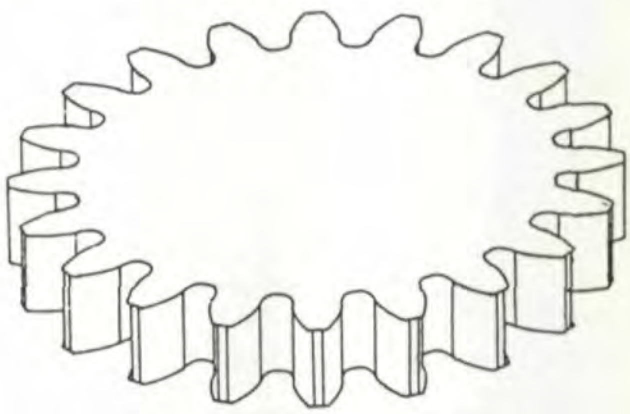

Fig. 13 – Perspective view of a gear with an automatically generated profile.

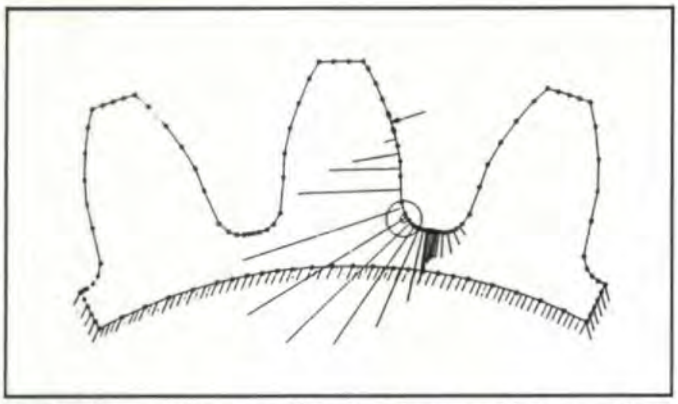

Fig. 14 – Automatically generated boundary element model of a non-undercut gear.

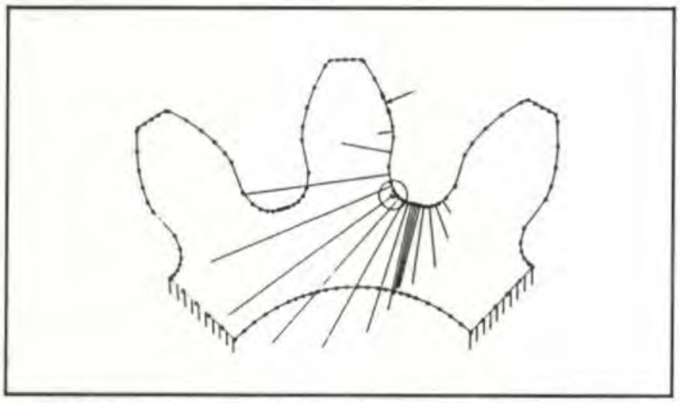

Fig. 15 – Automatically generated boundary element model of a severely undercut gear.

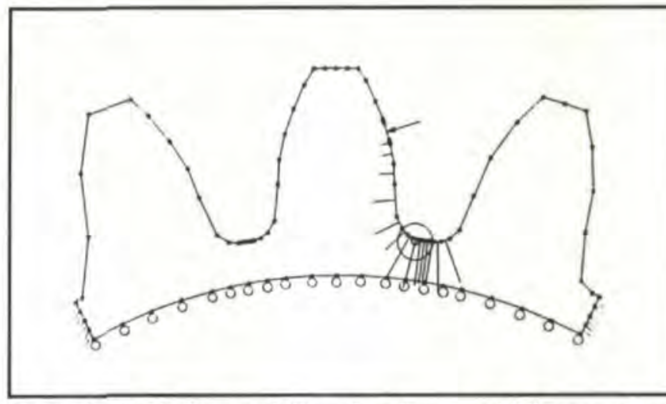

Fig. 16 – Automatically generated boundary element model of a non-undercut gear supported on rollers.

shows in perspective view a full gear with face width 0.3", which is being generated by the simple hob described before.

b) Generation of Boundary Element Meshes for Strength Computations: The estimation of the strength of a gear can be carried out in many different ways, of which the boundary element method is probably the most efficient and convenient. Because the boundary element method is very accurate, the stress concentration at the fillet of the gear tooth root is very sensitive to the correctness of the geometry of the fillet at the root of the gear tooth. The automatic gear profile generation procedure described in this article is very useful in generating boundary element models which accurately model the root geometries.

As described in an earlier article by Vijayakar and Houser, [4] the boundary element procedure can easily display stress variation along the boundary of the gear model, determine the location at which critical stresses occur and determine the AGMA geometry factor. The procedure also allows the computation of the state of stress at any prescribed point within the gear.

Several boundary conditions can be applied in the boundary element model of the gear teeth. The inner boundary and the sides can be fixed, or the inner boundary can be free, while the sides can be fixed, or else the inner boundary can be supported on rollers with the sides fixed. Figs. 14, 15 and 16 show the stress distribution along the boundaries of three thin-rimmed gears with different boundary conditions. The gear shown in Fig. 14 has no undercutting, and its inner rim and the sides are fixed, while the gear in Fig. 15 is severely undercut and has rigid side supports. Fig. 16 shows the stress distribution of another thin-rimmed gear with roller supported inner boundary and fixed sides.

c) Contact Analysis of Gears: Developments in the area of contact analysis of finite element models with friction have made it possible to determine the load dependent transmission error of gears in mesh by meshing finite element models of a pair of gears and turning them against each other in a simulation. However, the magnitude of the transmission error itself is typically very small.

Therefore, in order to carry out meaningful simulations of gears in mesh, where the error in the transmission error due to the finite element discretization of the gear profile is much smaller than the actual transmission error, it is imperative that the finite element model be able to model the geometry of the gear with a high degree of accuracy. In such a case, manual methods of model creation, such as using drawings and a digitizing tablet, are out of the question, and an automatic procedure such as that described in this article becomes essential.

As an example, consider a gear with 20 teeth, a diametral pitch of 10 per inch and a face width of one inch. Under a load of 1000 lb-inches, the load dependent transimission error of two such gears in mesh is of the order of 0.05°. If finite element contact analysis is to be used, the error in the transmission error due to profile discretization should be kept as low as 0.001°. Fig. 17 shows a part of the tooth profile that has been discretized. Let r_c be the radius of curvature, l be the length of the side of a typical element and ϵ be the discretization error. Then,

$$\epsilon = \frac{r_c\,(\theta/2)^2}{2} = l^2/(8r_c)$$

approximately. If we consider the part of the profile near, say, the pitch point, then the radius of curvature is

$$r_c = r_p \sin\phi = \frac{z}{2D_p}\sin\phi$$

where r_p is the pitch circle radius, ϕ is the pressure angle, z is the number of teeth and D_p is the diametral pitch. The length l of the side of a typical element is approximately

$$l = \frac{(A+B)}{D_p n},$$

where A and B are the addendum and dedendum constants of the gear, and n is the number of elements that the profile of the gear tooth spans. Therefore, the discretization error ϵ is

$$\epsilon = \frac{(A+B)^2}{4n^2 z D_p \sin\phi},$$

and the error δ in the transmission error is

$$\delta = \epsilon/r_p = \frac{(A+B)^2}{2n^2 z^2 \sin\phi} \text{ radians}$$

For δ to be of the order of 0.001° or 1.75×10^{-5} radians, the number of elements along the profile has to be n=30, and the coordinates of the nodes along the profile have to be at least as accurate as $\epsilon = 1.75 \times 10^{-5}$".

Figs. 18 and 19 show the finite element model of two gears in contact whose profiles were generated automatically by the procedure described in this article. Each gear has 32 nodes along each tooth profile.

The input gear was rotated at a constant angular speed, and a predetermined torque was applied on the output gear. Contact forces including the frictional and compressive components were computed for each position using a procedure [5] based on the Simplex algorithm, and transmission error and load-sharing information was obtained. Fig. 20 shows the computed transmission error for three different combinations of load torque M_o and frictional coefficient μ. An exaggerated value of 0.3 is chosen for the coefficient of friction to illustrate its effect on the transmission error. The transmission error curve for the light load shows ripples which may be attributed entirely to the discretization error in the profiles. In the curves for higher load, the same ripples reappear at the same places, but are much smaller than

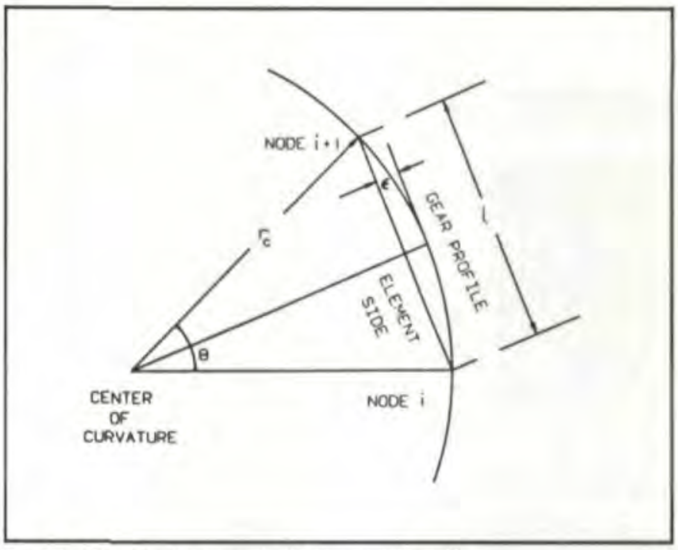

Fig. 17 – Discretization error in the gear tooth profile.

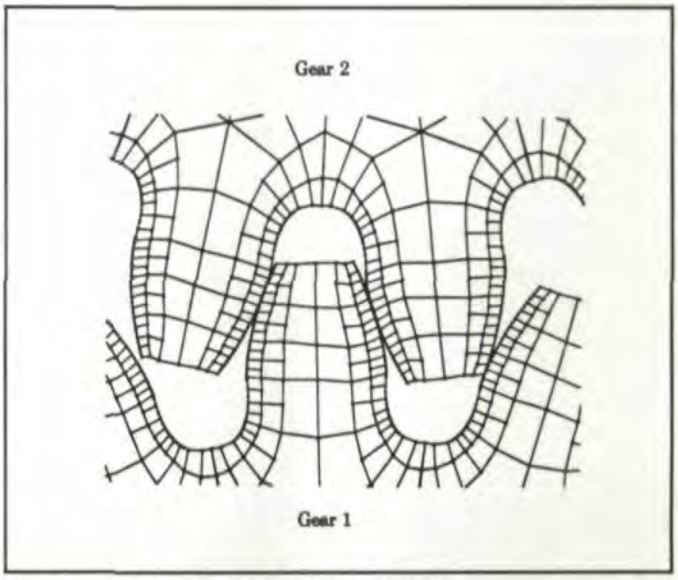

Fig. 18 – Finite element model for contact analysis.

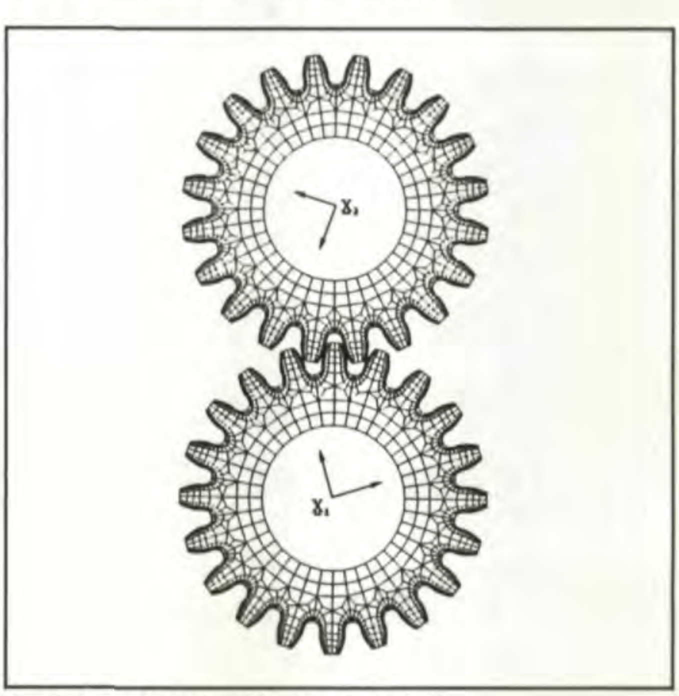

Fig. 19 – Finite element model for contact analysis.

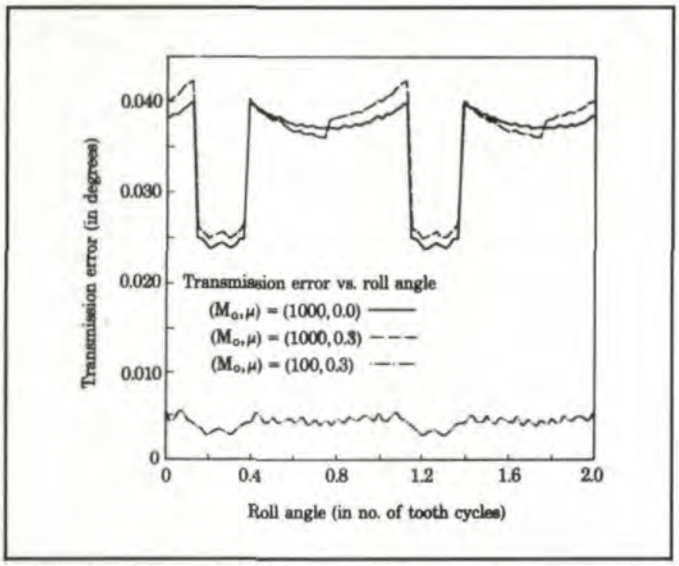

Fig. 20 – Transmission error curves obtained from finite element analysis.

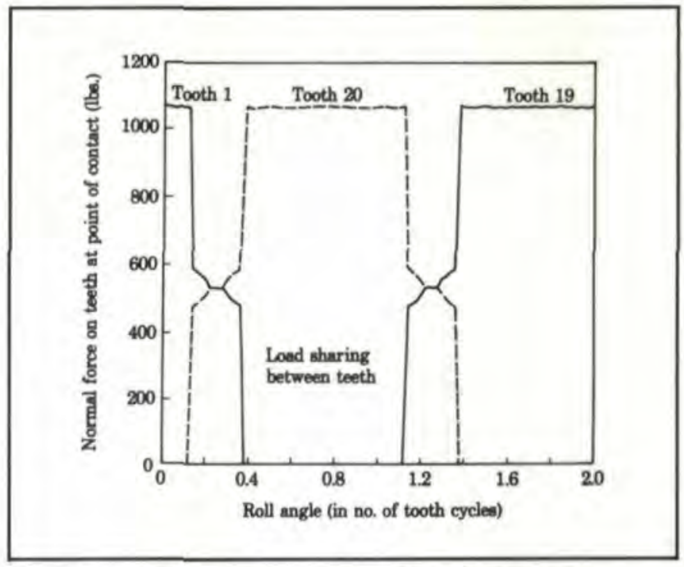

Fig. 21 – Load sharing curves obtained from finite element analysis.

the overall transmission error. Fig. 21 shows the load sharing between teeth as the gears roll through.

Conclusion

A simple, yet very general, procedure that can handle undercut as well as nonundercut gears has been described in this article. An important advantage of the method as implemented is that it is very easy to include any kind of modifications on the rack without changing the general structure of the procedure. The method has been tried out on practical applications, and the authors feel that it can be used to advantage whenever an accurate numerical description of generated gear tooth profiles is needed. A FORTRAN program has been successfully run on both an IBM PC and a VAX-11.

References

1. COLBOURNE, J.R., *The Geometry of Involute Gears,* Springer Verlag, 1987.
2. CHANG, S.H., HUSTON R.L., and COY, J.J. "A Computer Aided Design Procedure for Generating Gear Teeth", ASME Paper No. 84-DET-184.
3. HEFENG, BAI, SAVAGE, MICHAEL and KNORR, RAYMOND JAMES, "Computer Modeling of Rack-Generated Spur Gears", *Mechanisms and Machine Theory,* 20 (1985), pp. 351-360.
4. VIJAYAKAR, SANDEEP M. and HOUSER, DONALD R. "The Use of Boundary Elements for the Determination of the Geometry Factor", *Gear Technology,* Vol. 5, No. 1, Jan-Feb, 1988, pp.7ff.
5. VIJAYAKAR, SANDEEP M., BUSBY, HENRY R. and HOUSER, DONALD R. "Linearization of Multibody Contact", to appear in *Computers and Structures,* Pergamon Press, Oxford, England.

Acknowledgement:

Reprinted with permission of American Gear Manufacturers Association. The opinions, statements and conclusions presented in this article are those of the authors and in no way represent the position or opinion of the AMERICAN GEAR MANUFACTURERS ASSOCIATION.

The authors would like to thank the sponsors of the Gear Dynamics and Gear Noise Research Laboratory for their encouragement and financial support which made this study possible.

The Elementary Theory for the Synthesis of Constant Direction Pointing Chariots (or Rotation Neutralizers)

Cemil Bagci,
Tennessee Technological University
Cookeville, TN

Abstract:

Chariots with figures pointing in a fixed direction as they move, otherwise known as rotation neutralizers, are built with differential gear trains. Examples, such as the south-pointing chariot at the Smithsonian Institution and its replica, the Ohio State University-pointing-rotating-trophy-award-chariot, have been fascinating mechanical system designers for a long time. This article offers the design equations for the synthesis of such chariots and their engineering applications.

Introduction

The south-pointing chariot exhibited at the Smithsonian Institution, Washington, D.C., (circa 2600 BC) is shown in Fig. 1. Although the mechanism is ancient, it is by no means either primitive or simplistic. The pin-tooth gears drive a complex system, wherein the monk on the top of the chariot continues to point in a preset direction, no matter what direction the vehicle is moved, without a slip of the wheels.(1)

The south-pointing chariot is more than a historical curiosity. While the vehicle in Fig. 1 is a demonstration model, the mechanism has many practical engineering applications. It can be used where mobile or adjustable reference or tracking planes are required, such as in instrumentation where constant direction must be maintained; in light or signal beams to be positioned in preset directions; in rotary gravitational test chambers where one, clear directional view must be provided; and in rotary systems where reference planes must be maintained in preset positions.

When connected to the base or revolute joints of a robot,

Fig. 1 – The south pointing chariot exhibited at the Smithsonian Institution, Washington, D.C.

such a system will orient a coordinate reference plane in its originally set position to form a base for output of position sensors. It can move the reference plane with a sine function, retaining it parallel to itself, an application useful for tracing and machining circular paths and cylindrical and toroidal surfaces, welding and the laser machining of shell surfaces by the incorporation of a parallelogram linkage loop as illustrated in Fig. 9.

Design Equations

The constant-direction-pointing chariot is driven by a planetary gear train differential whose train value is (-1).[2] Fig. 2 shows a bevel gear planetary gear train differential having the train value of (-1). It is used in the rear end differentials of vehicles. Figs. 3 and 4 show two other planetary gear differentials generating the train value of (-1), but using spur gears. In these systems, let n designate the speed of a shaft and n_a the speed of the arm. A train value of (-1) means that when the planet arm is held stationary, $n_a = 0$, and when the first gear (gear 2) is rotated one revolution in one direction, $n_2 = 1$, the last gear (gears 5, 6 and 8 in Figs. 2, 3 and 4, respectively), rotates in the opposite direction one revolution, $n_5 \equiv n_6 \equiv n_8 = -1$ in these figures.

The equations of motion for a planetary gear train in general form are[2]

$$e = \frac{n_L - n_a}{n_F - n_a} \tag{1}$$

e being the train value defined by

$$e = (-1)^q \frac{\Sigma\,\mathrm{PDVER}}{\Sigma\,\mathrm{PDVEN}} \tag{2}$$

where Σ PDVER is the product of all the driver gear tooth numbers starting with the first gear considered, and Σ PDVEN is the product of all the driven gear tooth numbers, including the last gear. They are formed by keeping the planet arm stationary. The number of external contacts of the gears in the train is q; n_F, n_a and n_L are the speeds of the first gear, planet arm and the last gear in the train. See detailed applications of Equations 1 and 2 for the analysis and synthesis of simple and compound planetary gear trains and automatic vehicle transmissions in Reference 2. Let N_i be the tooth number of the ith gear. In Fig. 2 tooth numbers of gears satisfy $N_2 = N_5$; N_4 is of any practical number greater than 18 for efficient operation, and

$$e = -\frac{N_2 N_4}{N_4 N_5} = -1 \tag{3}$$

AUTHOR:

DR. CEMIL BAGCI *is professor of mechanical engineering at Tennessee Technological University, Cookville, TN, where he teaches courses and conducts research in machine design, kinematics, and robotics. Dr. Bagci studied at Technical Teachers College, Anakara, Turkey, and received his undergraduate and graduate degrees from Oklahoma State University, Stillwater, OK. He is author of over 150 technical papers and the recipient of numerous research awards. He is a member of AGMA, ASME and several other technical societies.*

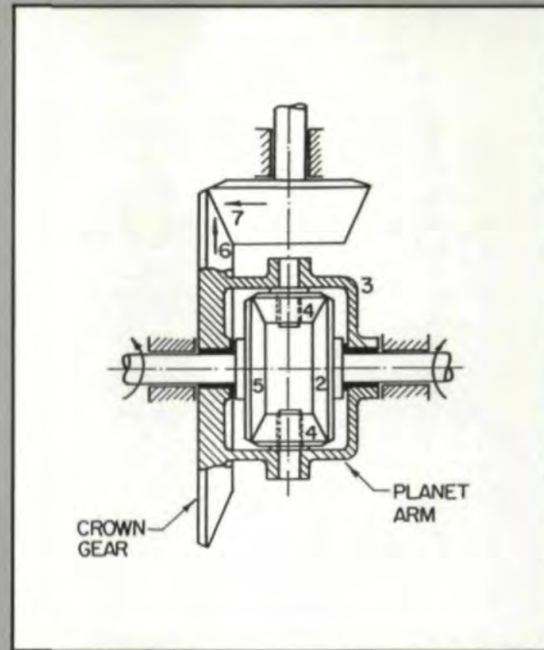

Fig. 2 – Bevel gear planetary gear train differential of train value (-1).

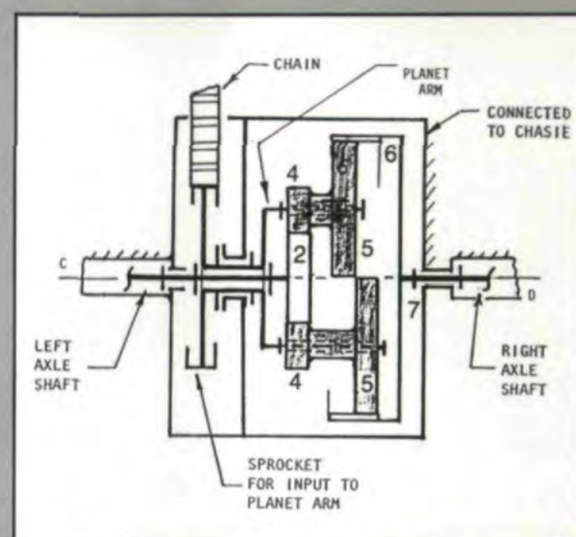

Fig. 3 – Spur gear planetary train differential with an internal gear and train value of (-1).

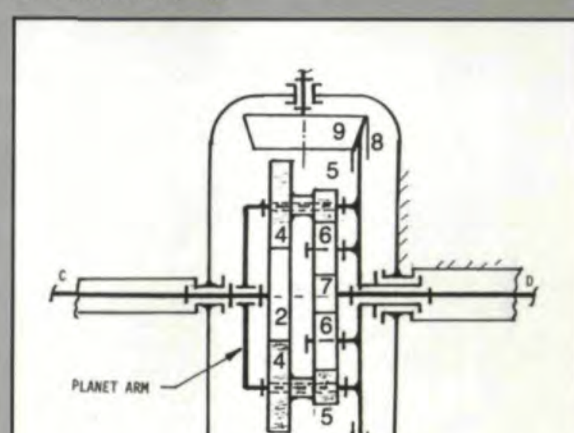

Fig. 4 – Spur gear planetary gear train differential with all external gears and train value of (-1).

In Fig. 3, for example, with tooth numbers $N_2 = 40$, $N_4 = 20$, $N_5 = 60$ and $N_6 = 120$,

$$e = \left(-\frac{N_2}{N_4}\right)\left(\frac{N_5}{N_6}\right) = -1 \tag{4}$$

In Fig. 4 with $N_2 = N_4 = 60$, $N_5 = N_7 = 20$, and $N_6 = 40$

$$e = \left(-\frac{N_2}{N_4}\right)\left(-\frac{N_5}{N_6}\right)\left(-\frac{N_6}{N_7}\right) = -1 \tag{5}$$

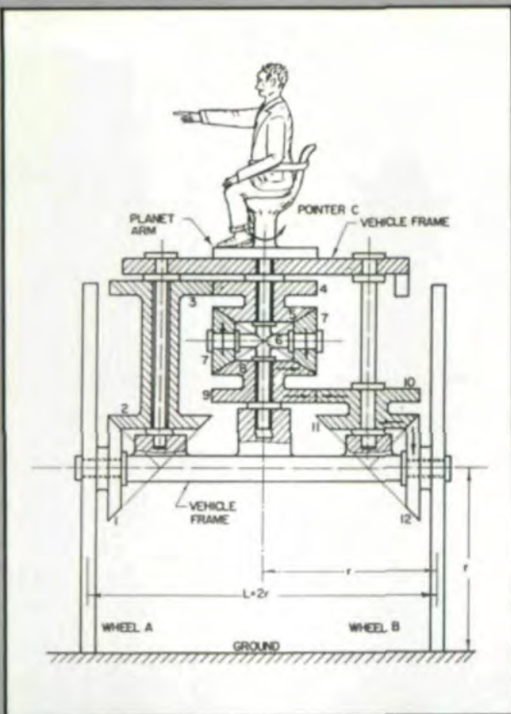

Fig. 5 – The form of the constant direction pointing chariot.

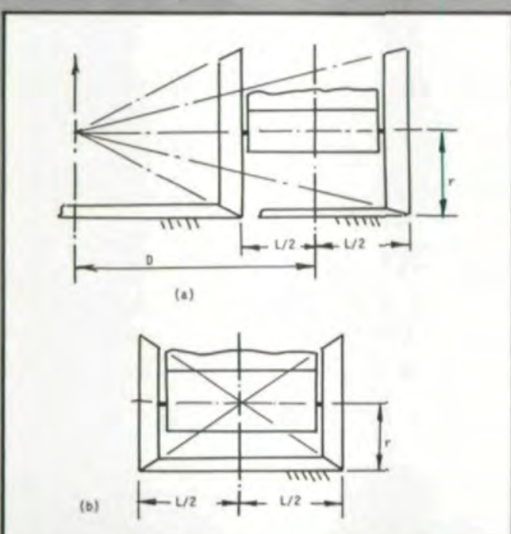

Fig. 6 – Wheels rolling on crown gear platforms.

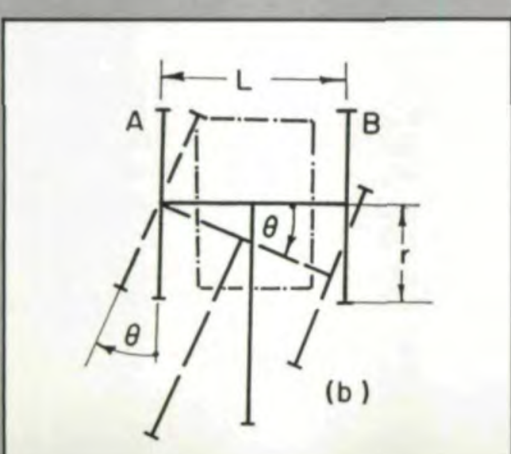

Fig. 7 – Chariot rotated through θ about the point of contact of wheel A.

Fig. 5 shows the skeleton of the constant direction pointing chariot, where the bevel gear differential of Fig. 2 is used. Bevel gears 8, 7 and 5 correspond to the bevel gears 2, 4 and 5 in Fig. 2. $N_3 = N_4 = N_9 = N_{10}$ for the spur gears, and $N_1 = N_2 = N_{11} = N_{12}$ for the bevel gears that transform the motions of the wheels to the first and last gears of the bevel gear differential gear train of gears, 5, 7 and 8. In precision machines and instrumentation systems for low torque applications, when the chariot is moving on a platform, wheels at A and B may have point contact on the platform, and they are compressed against the platform surface to cause proper level of traction as seen in Fig. 8. For large torque applications, when the chariot rotates about a fixed vertical axis, wheels are bevel gears rolling on a stationary crown gear to eliminate slip as shown in Figs. 6 a and b.

The function of the two-wheel, 12-gear mechanism is to keep the pointer or the planet arm of the differential gear train stationary with respect to the platform (ground) regardless of the direction in which the vehicle travels. The constant direction pointer is connected to the planet arm with an adjustable coupling, permitting repositioning of the pointer as desired. Let the radii of the wheels be r. They are positioned from the center of the chariot at equal distance L/2. Consider the rotation of the chariot through angle θ about the vertical axis passing through the contact point of wheel A. (See Fig. 7.) Gears 1, 2, 3, 4 and 5 remain stationary, and $n_5 = 0$. The vehicle frame has rotated through θ (with the pointer if wheel B did not rotate), but wheel B rolls on a circle of radius L causing gear 12 to rotate through

$$n_{12} = \frac{L\theta}{r} \tag{6}$$

This rotation causes gear 8 to rotate in relation to the vehicle frame through

$$n_8 = -\frac{L\theta}{r} \tag{7}$$

Applying Equation 1 using $n_L = n_5 = 0$, and $n_F = n_8$ we have

$$-1 = \frac{0 - n_a}{-\frac{L\theta}{r} - n_a} \tag{8}$$

and

$$2n_a = -\frac{L}{r}\,\theta \tag{9}$$

Since the planet arm must rotate through $(-\theta)$ about the vertical axis to maintain the fixed position of the pointer, Equation 9 suggests that

$$r = L/2 \tag{10}$$

must be satisfied in the design of the chariot. Then,

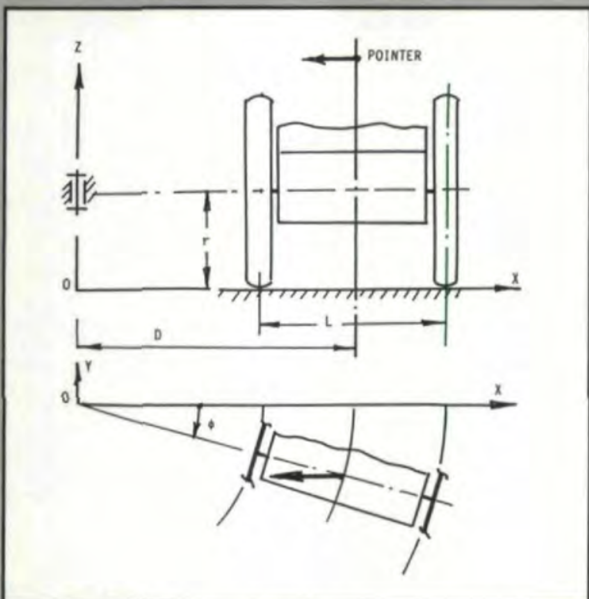

Fig. 8 – Chariot rotated through ϕ about a pole axis OZ.

$$n_a = -\theta \tag{11}$$

neutralizing the pointer rotation.

Let us observe more general motion of the chariot. Let it be rotated through ϕ about a vertical pole axis OZ at some distance D from the center of the chariot. (See Fig. 8.) The wheel A experiences rotation

$$n_1 = n_5 = \frac{D - \frac{L}{2}}{r}\,\phi \tag{12}$$

On the other hand, wheel B experiences rotation

$$n_{12} = -n_8 = \frac{D + \frac{L}{2}}{r}\,\phi \tag{13}$$

Substituting n_5 and n_8 into Equation 1 we again find

$$-1 = \frac{\dfrac{D - \frac{L}{2}}{r}\,\phi - n_a}{-\dfrac{D + \frac{L}{2}}{r}\,\phi - n_a} \tag{14}$$

and

$$2n_a = -\frac{L}{r}\,\phi \tag{15}$$

with

$$r = L/2 \tag{10}$$

$$n_a = -\phi \tag{16}$$

Therefore, the pointer is undisturbed wherever the chariot goes without the slip of wheels.

In addition to positioning planes or directing light or signal beams in preset directions, the chariot can be used with a parallelogram linkage loop and extended links to function as a tracer of exact circles of both large and small radii, where the use of wormgear or ordinary gear drives may be considered very costly. In that form, it can carry cutter to machine, grind, cut with a laser beam or weld inner surfaces of shells and large bearings. (See Fig. 9, where 0 is the center of the planet arm, OE is the constant direction pointer, EP is the task performing link such as an end-effector link of a robot, OG=EF and GF=OE.) In this form EP is normal to the shell surface, and it can be extended to the desired size of the machined surface, (D+EP) being its radius. Tools are mounted on vertical extensions to retain the chariot outside the shell surface. The platform (or crown gear) on which the wheels rotate is moved in the vertical direction for machining or task feed. If full rotation of the chariot about the vertical axis is required, a second parallelogram loop (OHIE) is added with $60° \leq \beta \leq 120°$ so that each loop moves the other parallelogram loop from its dead center position. Forming EP'

EDITORIAL

(continued from page 5)

to give presidential access to the national treasury to this man? One has the nagging feeling, on studying Mr. Bentsen's record, that he could put himself first, Texas second and the country third — not exactly the priorities we'd like to see in a potential president.

Mr. Bush's running mate, Dan Quayle, seems much more a liability than an asset to the campaign and has a long way to go to achieve presidential stature. It's not his youth that's a problem; both Theodore Roosevelt and John Kennedy were within a year of his age when they assumed the presidency. It's the sense that he is untried, unaccomplished, inexperienced and, yes, immature.

Mr. Quayle is a charming and attractive man, apparently one of Nature's darlings. Thanks to a cushion of family wealth and influence, he has coasted easily to the right places at the right times to get into college and law school; to get the good jobs and make the right acquaintances; and to have the best chances without having to have the backup credentials demanded of others. He has also benefitted from the generosity of lobbyists, being ranked 15th in the Senate in the amount of money earned from honorariums for speeches, articles, travel expenses and lobbyists' golf outings. This puts him well above the amount earned by numerous more experienced, better known politicians — including his running mate and his two opponents, who take no such fees at all. For a man to whom much in life has come easily, the remark that he should not be judged harshly for a decision made when he was young and under pressure is both disturbing and revealing. He needs to be reminded of the sign on the President's desk that says, "The buck stops here."

Fairness demands that we remind ourselves that an unpromising candidate does not necessarily make a bad president. Popular wisdom in 1860 was that the man from Illinois was a rube and an amateur, a good choice for the bosses because he could be easily manipulated. Abraham Lincoln proved popular wisdom wrong, and he is not the only man of less-than-obvious presidential stature to grow into the job. Maybe the country will be as fortunate again.

But the disturbing question remains, why is it that in the last twenty years, our national search for presidential timber too often seems to yield nothing but twigs? The people with real character, leadership ability and vision for the future don't seem to want to run. Those who do want to run seem less than the best.

I don't know what the answer is. Maybe there isn't one— or at least not a simple one. I do know that it is demoralizing for individual citizens and bad for a country to have election after election where the best candidate is "None-of-the-Above."

Michael Goldstein
Editor/Publisher

on the reverse side and mounting cutters on vertical extensions, the chariot-linkage system performs operations on the outside surfaces of shells, wheels and shafts. If the platform is tilted like a swash plate about a horizontal axis, JK for example, P can machine a toroidal surface.

The chariot rotating about a pole as in Figs 8 and 9 can be used in rotating roller coasters in which the passengers always look in one desired direction.

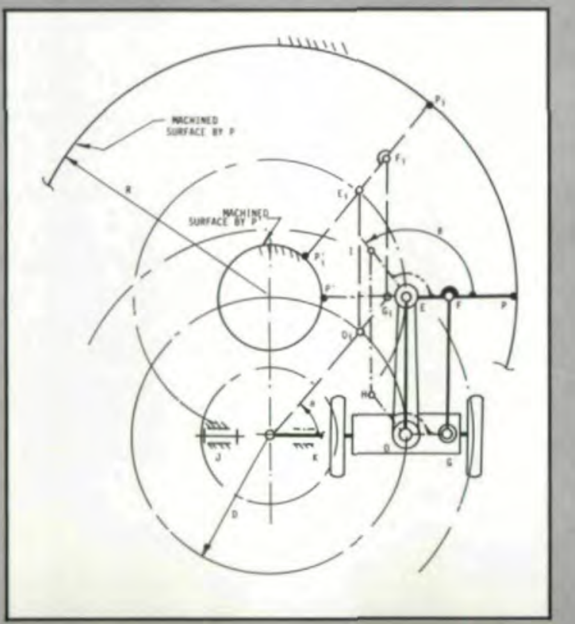

Fig. 9 — Chariot with parallelogram linkage loops performing tasks on cylindrical and toroidal surfaces.

Conclusions

In the foregoing discussion, the simple equations of motion for the ever-puzzling constant-direction-pointing chariots are given. They can easily be designed for machining, robotics, roller coaster and instrumentation applications. The parameters that must be observed are as follows: $r = L/2$, $N_3 = N_4 = N_9 = N_{10}$, $N_1 = N_2 = N_{11} = N_{12}$. The differential gear train driven with gears 4 and 9 has train value of (-1). Although the bevel gear planetary gear train differential is shown in Fig. 5, one can replace it with the spur gear planetary gear train differentials shown in Figs. 3 and 4, where gears 4 and 9 in Fig. 5 are connected to the C and D shafts of the first and last gears of the spur gear differentials. Chain and crown gear driven planet arms are connected to the pointer. Chariots with parallelogram linkage loops and tilting platforms offer precision task performing systems on cylindrical and toroidal inner and outer surfaces. Many other industrial applications of the constant direction pointing chariots are limited only by the ingenuity of the designer.

References

1. DUDLEY, DARLE W., *The Evolution of the Gear Art*, AGMA, 1969.
2. BAGCI, C., "Efficient Method for the Synthesis of Compound Planetary Differential Gear Trains for Multiple Speed Ratio Generation," Proceedings of the 10th Applied Mechanisms Conference, December 6-9, 1987, New Orleans, LA.

BACK TO BASICS...

Basic Spur Gear Design

William L. Janninck
Illinois Tools Division, ITW Inc.
Lincolnwood, IL

Primitive gears were known and used well over 2,000 years ago, and gears have taken their place as one of the basic machine mechanisms; yet, our knowledge and understanding of gearing principles is by no means complete. We see the development of faster and more reliable gear quality assessment and new, more productive manufacture of gears in higher material hardness states. We have also seen improvement in gear applications and design, lubricants, coolants, finishes and noise and vibration control. All these advances push development in the direction of smaller, more compact applications, better material utilization and improved quietness, smoothness of operation and gear life. At the same time, we try to improve manufacturing cost-effectiveness, making use of highly repetitive and efficient gear manufacturing methods.

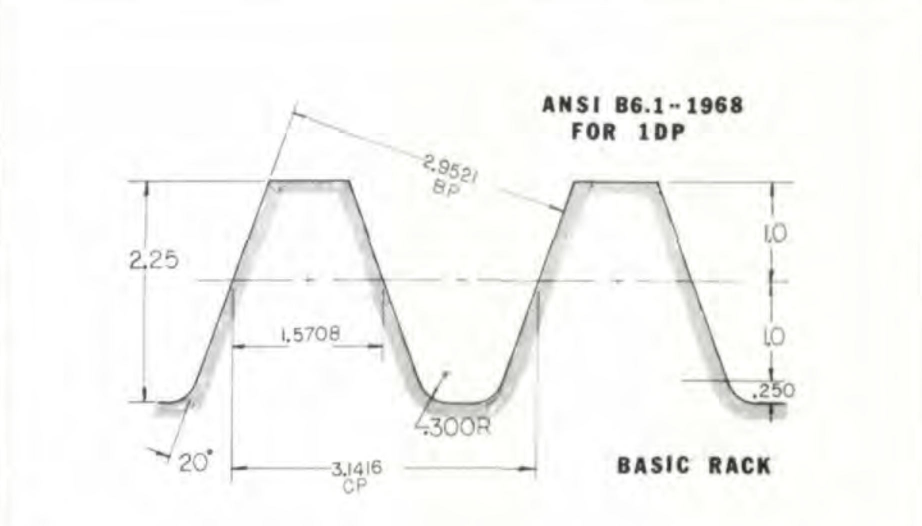

Fig. 1

All these considerations make for a bewildering number of parameters to work with. The novice or aspiring gear designer should not be overwhelmed by the many details involved, but gradually absorb as much basic gear related information as possible concerning any and all aspects of gearing. Eventually the overall picture of gear applications, design, qualification and manufacture will come into focus.

In discussing the basics of gear design we shall use an example of the simpler geometrical case of spur or straight tooth parallel axis gears. Almost all of the basics are similar in other forms of gearing, such as helical and herringbone gears in a parallel axis arrangement and crossed axis helicals, bevel and worm gearing in the intersecting axes or skew axes arrangements. The details and geometry will vary, but the major concerns are quite similar.

The Basic Rack

The basis for specifying gear teeth, the starting point for gear specification, is geometrical in nature and can be layed out in a diagram of the gear tooth form as if

AUTHOR:

W. L. JANNINCK *is a gear geometrician and consultant to the Illinois Tools Division of ITW Inc. He has experience in the design and application of both generating and forming type metal cutting tools, specializing in the area of tooling and gaging for the manufacture of gears, splines and sprockets. Prior to entering private practice, he was manager of product engineering and chief engineer at ITW. He has served on various committees of the AGMA and MCTI and is chairman of the AGMA Cutting Tool Committee. He also served on the SAE-ANSI Committee on Power Transmission Chains and Sprockets. He has written extensively on tool applications, gaging, gear design and gear inspection. He was educated at Northwestern University, Evanston, Illinois.*

the gear had an infinite number of teeth and were a rack. This concept is called the basic rack and differs for each tooth form system.

The current popular and widely used tooth form system for spur gears accepted worldwide is shown in Fig. 1. In the United States it is identified as the *ANSI B6.1 – 1968 Standard for Tooth Proportions for Coarse Pitch Involute Spur Gears.* Cutting tools to produce this tooth form in standardized diametral pitches are frequently carried in stock in gear cutting houses and tool supply firms.

The basic rack described here is far from the only one possible and in the archives, museums, text books and technical papers many others are found. At least 30 different basic forms of involute gears have been in popular use at some time. Forms by Brown & Sharpe, Grant, Sellers, Hunt, Logue, Willis, Day, Anderson, Parkinson, Nuttall, Fellows, Brown, Acme, Simmons, P&H, Wisdom, Maag, Sunderland and probably many more are sometimes still in use today, and the gear engineer should be aware of this gear lore. It is not unusual for a gear engineer to be asked to reproduce some of these old designs. While some of the tooth forms are now recognized as industry standards, many of the names of the originators have disappeared.

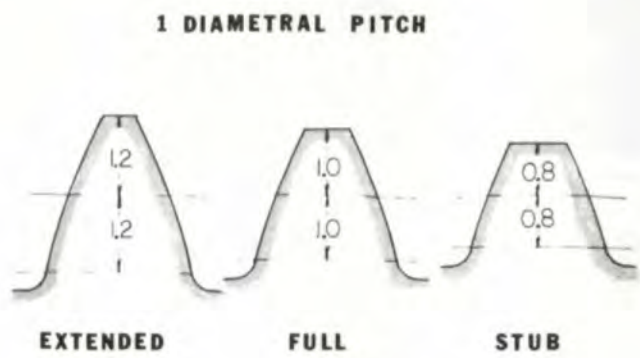

Fig. 2

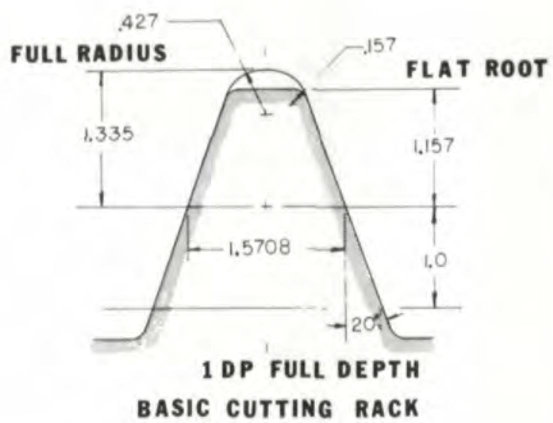

Fig. 3

Noninvolute Tooth Forms

Noninvolute form conjugate gearing systems, such as the cycloidal form, can also be used for gear building. Modified involute systems like the 14.5° composite system are also sometimes used. Other noninvolute systems include Williams, Wildhaber, Novikov and Concurve. In the field of fine pitch gearing a number of noninvolute form systems are used regularly. Many are of the ogival form and follow the British Standard or the Black Forest Standard. Some names include Prescott, Circular Arc and Wickenburg. These sets may be found in the clock, watch, instrument, timer and small toy trade.

These basic rack systems are referred to only for background, and we will not deal with the quite interesting aspects of these types of gears. They each have their place in mechanisms and should be recognized for that.

General Tooth Form Systems

In involute gearing there are three general tooth form systems. The three choices are full depth, stub depth and extended depth. (See Fig. 2.)

Full depth is probably the system of choice for most gear designers. It is specified using diametral pitch, an inch system. In this case, the addendum equals 1.0" for a 1 DP gear. The working depth equals 2", and clearance in the root area will vary as needed; in general, from a minimum of .157" to as much as .5".

Stub depth gears have been quite popular for several reasons. The most important one is increased strength. Another is the possible use of smaller gear tooth numbers in compact transmission boxes. In a stub gear, the gear addendum is less than 1.0" and, likewise, the working depth is less than 2.0" for a 1 DP gear. Usually the gear addendum and working depth are about 75% to 80% of the full depth format.

Extended depth is not nearly so well known or so popular, but it does exist, and some very interesting gearsets have been made with it. The applications include printing roll drives, where the gear inaccuracy can be spread over as many as

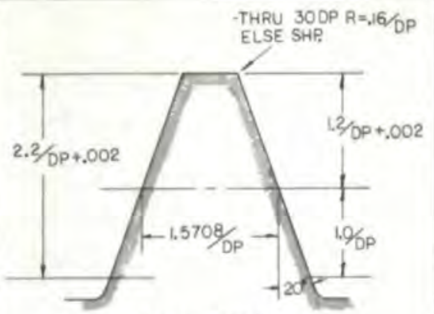

Fine Pitch

Fig. 4 Basic Cutting Rack

1 DP

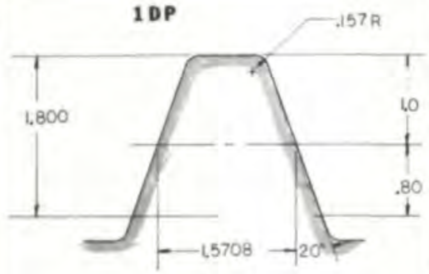

AGMA Stub

Fig. 5 Basic Cutting Rack

Fellows Stub

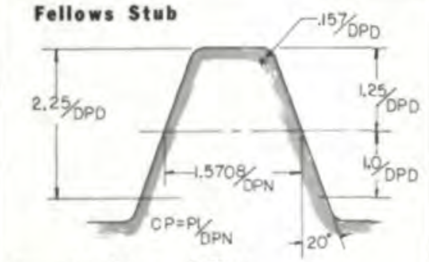

Example: 3/4 DP = DPN/DPD

Fig. 6 Basic Cutting Rack

three tooth pairs and will smooth the rotational transfer of motion. In other gear boxes, the extra depth which usually brings along with it an increased contact ratio, possibly of two or more, and finer pitch teeth, has been referred to as a "quiet gear set". Extra depth teeth do have a property referred to as gear tooth compliance or flexure because of the height of the teeth. Excessively long depth will cause increased problems in the manufacturing area. Although no official standards are published, working depths of 2.2, 2.4, 2.5 and 2.7 for a 1 DP basis have been seen in use.

FULL DEPTH SYSTEMS. Some of the standards in use today which may not all be published or officially adopted by a standards group are shown in Table 1.

A finishing basic cutting rack is defined as the complement of the basic rack for purposes of describing the tooling used to produce the gear form. Fig. 3 shows the basic cutting rack for a full depth system, comparing the flat root to the full radius or full fillet form for 20 PA. Fig. 4 shows the basic cutting rack standardized for fine pitch gears, that is, 20 DP and finer. It shows the special considerations given to get an increasing amount of clearance in the gear root as the teeth get very small. The .20/DP + .002 clearance is a larger proportionate amount at 100 DP than at 20 DP.

STUB SYSTEMS. The AGMA stub system shown in Fig. 5 has been very popular for many years for spur gears, particularly in industrial applications, and is also used as the standard tooth form for herringbone gears. Another interesting system is shown in Fig. 6. It is the combination or split pitch system and uses the circular pitch and circular tooth thickness from one diametral pitch and the addendum and whole depth from another. On a gear of 3/4 DP, for example, the gear is basically a 3 DP gear with the shorter addendum and whole depth for a 4 DP gear; hence, it is a stub form. Some caution should be used with this system of stub specification. 3/4 DP *has been mistaken for .75 DP, which is* substantially larger in size.

Extended depth systems, while widely used in certain areas of the gear industry, have never been adopted as an actual standardized tooth form. Extended depth systems are used in certain printing press applications and in some vehicle gearing.

Such systems might have the following specifications: PA, 20.0; Addendum, 1.2; Whole Depth, 2.65; Fillet Radius, .300.

OTHER TOOTH SYSTEMS. There are several ways to describe gears based on inch and metric measurements. For full depth we can specify the dimensions in four different ways.

1. Diametral Pitch. This is the ratio of gear teeth divided by the pitch diameter in inches. It is an inch system, and the dimensions for the gear data are calculated by dividing the specific basic rack values by the chosen diametral pitch. The diametral pitches are established in a list as recommended selection values.

2. Circular Pitch. The circular pitch of the gear is selected according to a recommended series, and the balance of dimensions is set in proportion to the chosen circular pitch by multiplying by the specific basic values. The proportions are the same as an equivalent diametral pitch gear, and then, if converted, the DP equals π divided by the circular pitch. There are applications where circular pitch spur gearing is still used today, and worm gear sets traditionally use the circular pitch to set the tooth proportions.

3. Inch Module. In the modular specification of gears, the module number is the addendum of the gear desired. A 1" module gear has a 1" addendum and, thus, is equivalent to a 1 diametral pitch gear. While modular inch gears are used occasionally, a series of recommended modules has not been published.

4. Metric Module. In the metric

Table 1 — Full Depth Systems

Name	PA	Addendum	Whole D.	Fillet R.
Flat Root	14.5	1.0	2.157	.157
Flat Root	20.0	1.0	2.157	.157
ANSI B6.1	20.0	1.0	2.250	.300
Full Fillet	14.5	1.0	2.440	.534
Full Fillet	20.0	1.0	2.335	.427
Full Fillet	25.0	1.0	2.250	.317
Fine Pitch	20.0	1.0	2.2+.002	Var.

Table 2 — Stub Systems

Name	PA	Addendum	Whole D.	Fillet R.
AGMA Stub	20.0	0.80	1.80	.157
Full Fillet	20.0	0.80	2.0	.500
Fellows Stub	14.5	1/DPd	2.25/DPd	.157/DPd
Fellows Stub	20.0	1/DPd	2.25/DPd	.157/DPd

DPn = DP Numerator DPd = DP Denominator Cir. Pitch = π/DPn module the addendum of the gear is specified in millimeters, and all other dimensions are likewise set in proportion to the addendum. It is a metric based system and a recommended series of modules are published. For a simple conversion, one can divide 25.4 by the metric module and arrive at the equivalent diametral pitch, and work from there if one is more comfortable with the DP system.

Fig. 7 shows a comparison of the four bases with relative sized gear teeth.

Symmetrical Rack Systems. The standard proportioned gear or "textbook" design is based on a symmetrical rack concept; that is, both gears in a set can be specified from a common rack system. From a practical standpoint, this permits the use of a single generating tool, hob or shaper cutter to produce a wide variety of mating gear sets. (See Fig. 8.)

Unsymmetrical Rack Systems. Most gear designs encountered today are based on the symmetrical system. In some instances asymmetry has been used. One example is obvious where the same strength material is used for both gear members and where the pinion is somewhat smaller than the gear. The beam strength of the gear is greater than that of the pinion. One way to bring the strength of both gears into balance is to increase the tooth thickness of the pinion and reduce that on the gear by an equal amount, keeping diameters and center distance unchanged. Special cutting tools are required for both the gear and the pinion. Fig. 8A illustrates an unsymmetrical rack application.

Natural Undercutting

As the number of teeth in a standard proportioned gear decreases, a point is reached where the phenomenon of natural undercutting occurs. For the standard 20 PA, full depth system, 2.25 WD and .300 fillet radius, this point occurs at 16 teeth and lower. The definition of natural undercut is the trimming away of a portion of the involute profile just above the gear base diameter by the rolling generating action of the cutting rack. The lower the number of the teeth being cut, the more the undercutting, until at nine teeth, insufficient involute is left to permit proper functioning of the teeth. In other words, the contact ratio is less than 1.0. Fig. 9 shows a chart comparing the

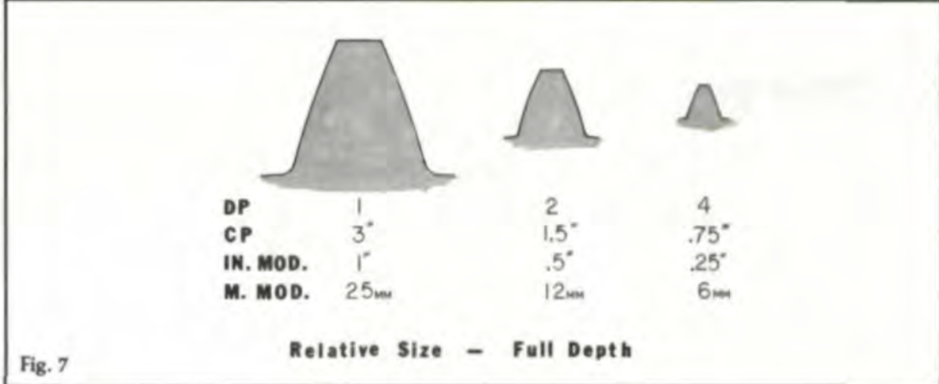

Fig. 7

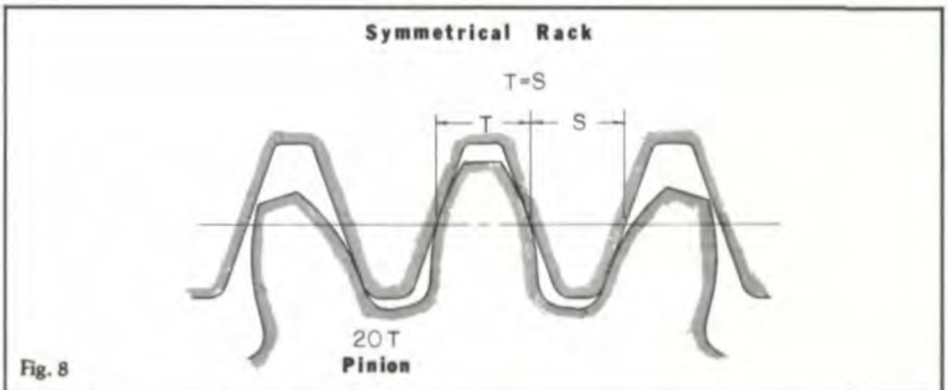

Fig. 8

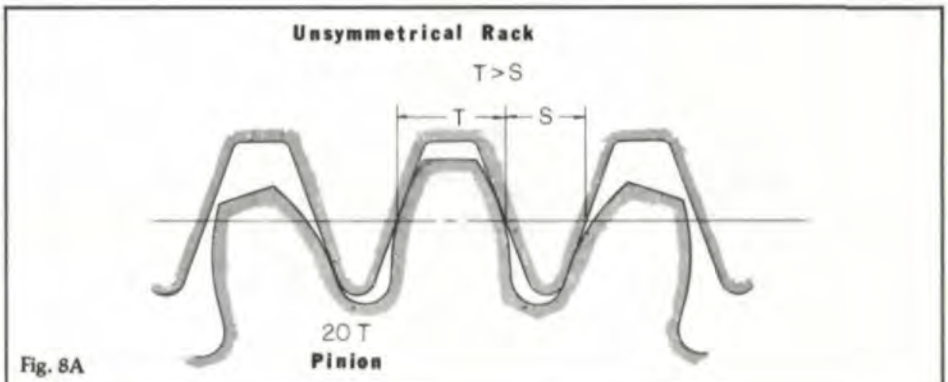

Fig. 8A

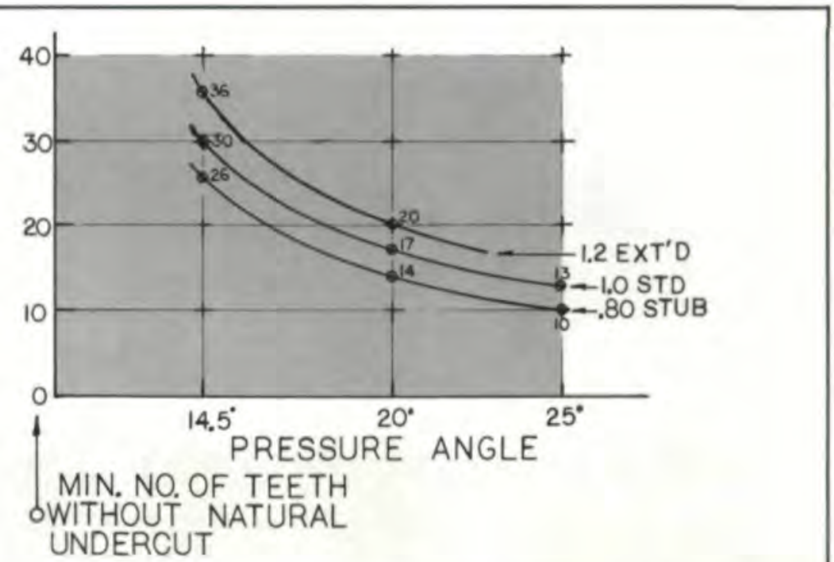

Fig. 9

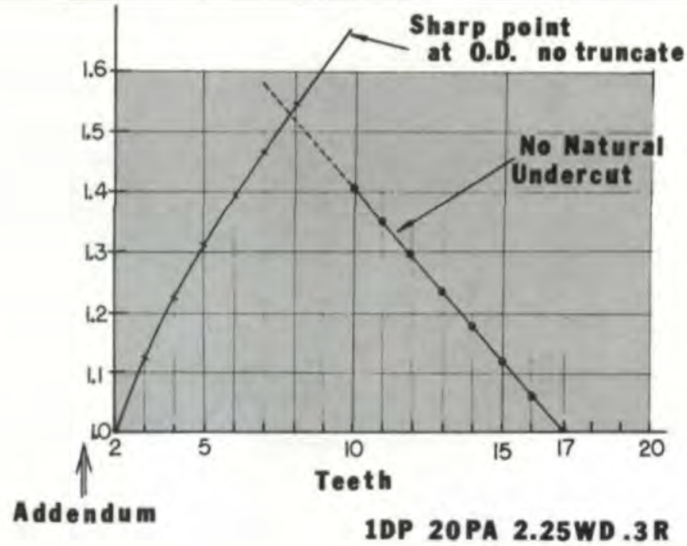

Fig. 10

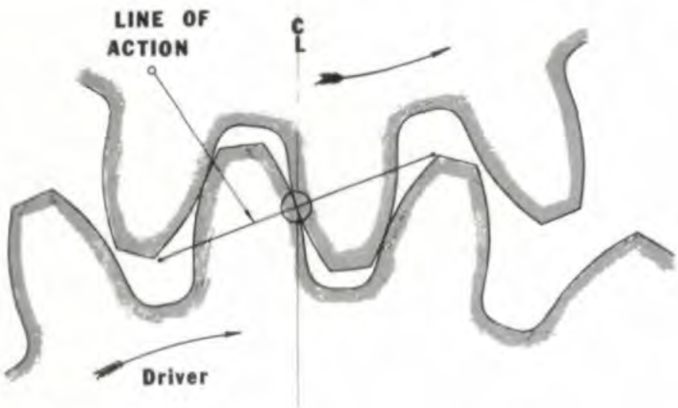

Fig. 11

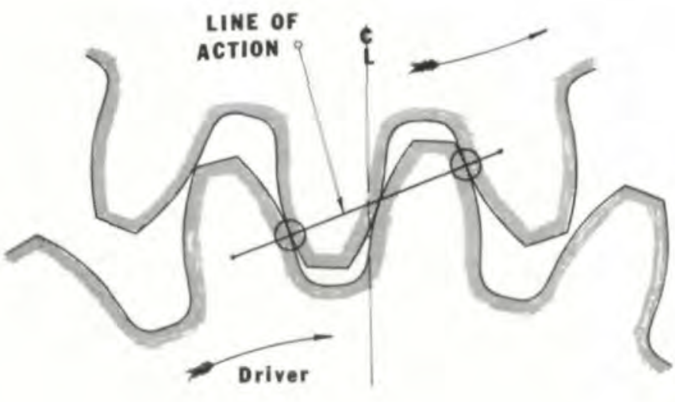

Fig. 12

number of teeth at which undercutting begins for various pressure angles and for .8 stub, 1.0 full depth and 1.2 extended depth.

Eliminating Natural Undercutting

Undercutting not only removes part of the involute but also reduces the strength of the pinion by thinning the base of the tooth. The use of enlarged, oversize or long addendum pinions is a way of reducing or eliminating the natural undercut. This is accomplished by holding the cutting rack out on the pinion, creating a long addendum and an increased tooth thickness, and then sinking the cutting rack in on the gear, creating a short addendum and a reduced tooth thickness. This approach holds the center distance at standard. An alternative to this approach is to enlarge the pinion and hold the gear at standard. Spread centers or non-standard centers are required for this set, and whenever the centers are non-standard, there is a change in the operating pressure angle, departing from the nominal gear set value. For external gears the operating pressure angle rises if the centers are spread and drops if the centers are closed.

Fig. 10 is a chart of the enlargement necessary to eliminate natural undercut.

Sharp Pointed Teeth

As the pinion is enlarged on diameter or the pinion cutting rack is shifted out, the tip flat at the outside diameter is reduced. If shifted far enough, the gear tip will eventually become sharp pointed and then, beyond that point, the gear outside diameter will be reduced or truncated, and the gear will have depth values below standard. The relationship of oversize addendum relative to achieving a sharp pointed pinion at the standard

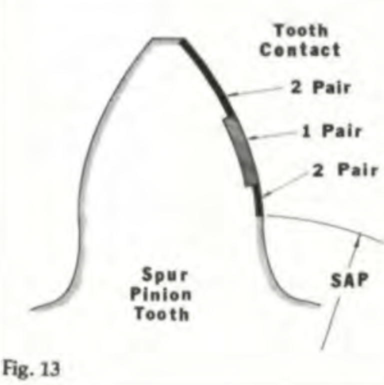

Fig. 13

whole depth without truncation is also shown in Fig. 10. A compromise may have to be made in some cases between undercutting and sharp pointed teeth if electing to work with small numbers of pinion teeth.

Contact Ratio

Contact ratio, which is the actual line of action divided by the base pitch, is a measure of the tolerance for passing the load supporting contact from the current pair of gear teeth to another succeeding pair. A contact ratio equal to 1.0 means a new pair of teeth pick up the contact transfer immediately after the old teeth separate from contacts with little back-up or insurance for the exchange.

A contact ratio below 1.0 means there is not enough involute surface available to make a timely exchange with proper angular rotation and, aside from inertial carry over, damaging edge contact can occur which is usually associated with gear noise.

A contact ratio greater than 1.0, such as 1.5, signifies that, for a substantial part of the time two pairs of gear teeth carry the load, and the balance of time only one pair of teeth carry the load. Fig. 11 illustrates the instant in time when there is only one pair of gear teeth in contact, and Fig. 12 shows another instant when two pair of teeth are in contact and supporting the load on a gear set with 1.556 contact ratio. Fig. 13 shows the progression of teeth pairs in contact across the active gear profile.

Gear Noise

Gear noise is frequently associated with the contact ratio and total tooth depth, the stub teeth being more prone to noise and at the same time relatively

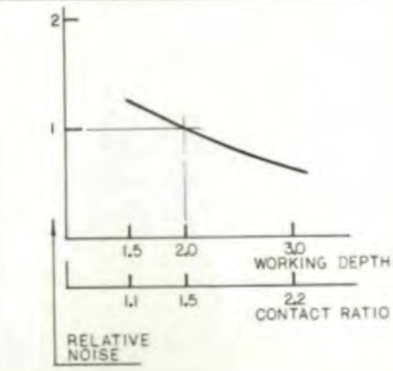

Fig. 14

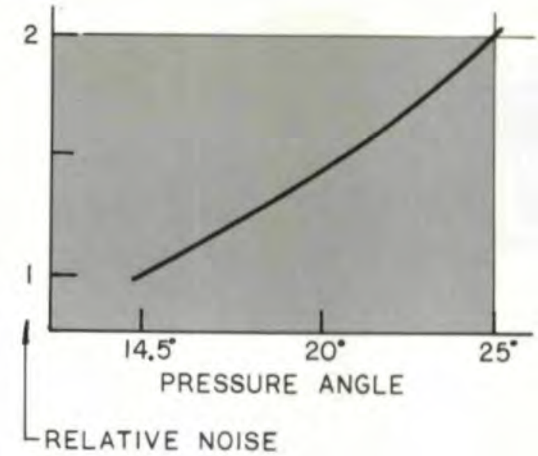

Fig. 15

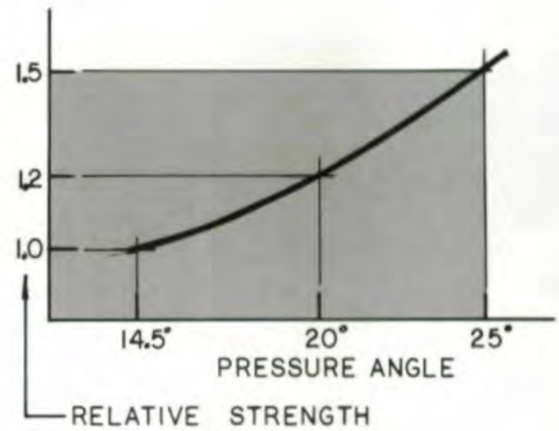

Fig. 16

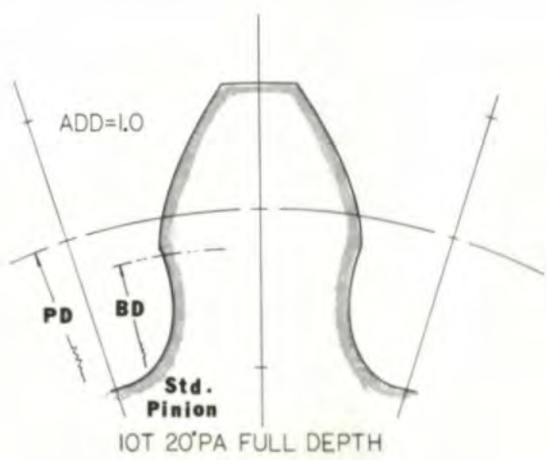

Fig. 17

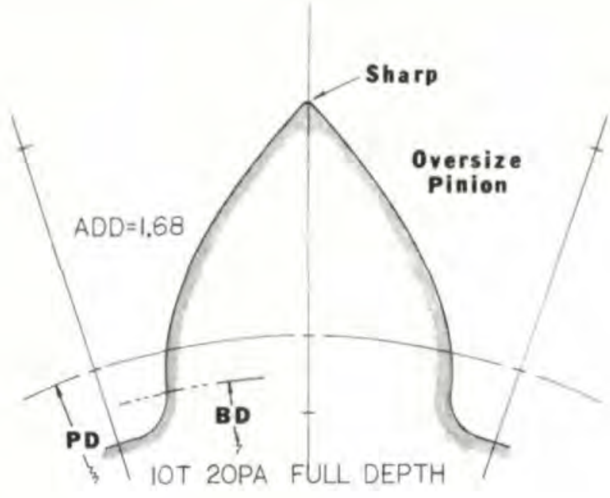

Fig. 18

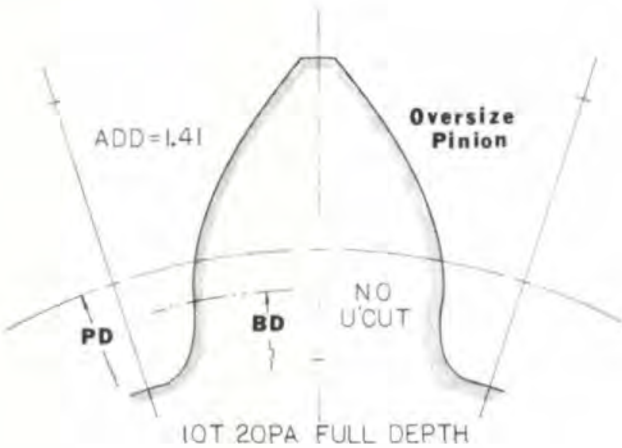

Fig. 19

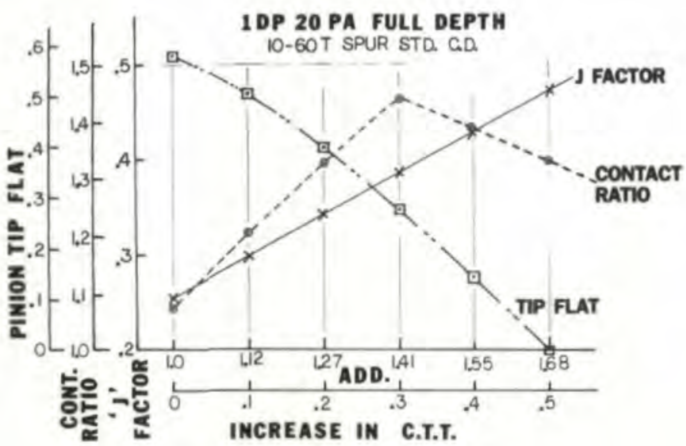

Fig. 20

lower on contact ratio. Extended depth teeth with higher contact ratios tend to be quieter. The graph in Fig. 14 illustrates this relationship.

Gears with lower pressure angles are also known to have lower noise levels and, because of their geometry, have higher contact ratios as graphically shown in Fig. 15.

Relative Strength

As the pressure angle goes up, the gear tooth bending strength goes up also, other things being equal. Likewise, as the pressure angle is reduced the strength is lessened. The relationship of the pressure angle and relative strength is shown in Fig. 16.

A Case Study

To focus on some of the generalities addressed, a sample spur gear set was constructed having a pinion of 10 teeth mating with a 60 tooth gear. If the standard 20 PA full depth 2.25 WD and a .300 fillet radius are used, a natural undercutting situation will occur. Fig. 17 is a scale form of the pinion generated with standard proportions using the above rack form. The addendum is 1.0 and the undercutting is visible just above the base circle.

In Fig. 18 the basic rack has been held out and the outside diameter of the pinion enlarged, creating an oversize pinion. The amount of oversize used is that necessary to reach a sharp pointed tip, but still retain the standard full depth without truncation. All signs of natural undercutting are gone. The addendum is 1.68.

Another approach was to make the pinion just enough oversize to eliminate the natural undercut, which only required an addendum of 1.41, a value readily found in the trade standards. Fig. 19 shows the form for the final design.

An interesting analysis of this gear set can be made by plotting pinion tip flat, contact ratio and "J" factor against the pinion addendum. This is presented in Fig. 20, a three variable graph. The tip flat is largest at standard addendum and decreases to zero at 1.68 addendum. At the same time, the "J" factor, which is a measure of strength, is increasing steadily. An interesting thing occurs with the contact ratio. It climbs as the pinion addendum increases, until at 1.41 addendum the contact ratio begins to decline.

The use of the 1.41 addendum represents a good compromise for all three variables.

Relative Sliding

As a pinion tooth passes through the mesh contact zone with its mating gear, the tooth surfaces pass over each other. Except for the point at the operating pitch circles where pure rolling exists, different lengths of involute surface on each mating gear sweep over each other and sliding occurs. This sliding is usually greatest near the pinion outside diameter, reduces to zero at the operating pitch diameter and reverses direction and continues to increase again to a maximum near the start of active profile. Of the standard proportioned gears, stub teeth have the least sliding and those using the extended depth have the most. Likewise long addendum gears have more sliding than standard addendum gears. In rating gears for durability, relative sliding is a factor and must be considered. Fig. 21 graphically illustrates, for our case study gear sets of 10 & 60 teeth, the comparison of involute segments at the tip of the pinion

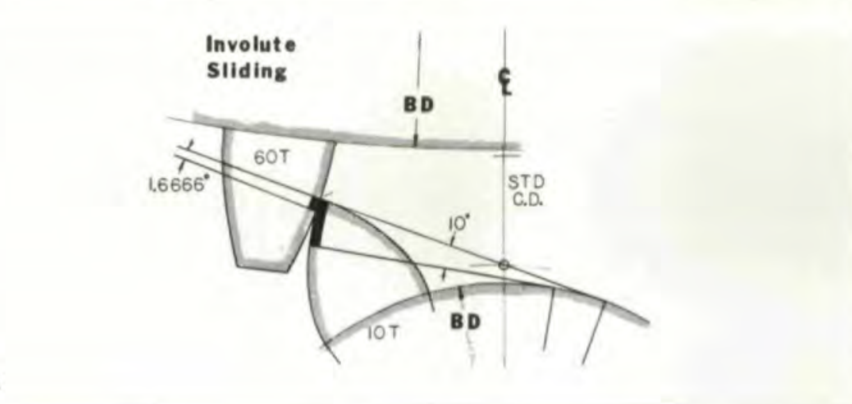

Fig. 21

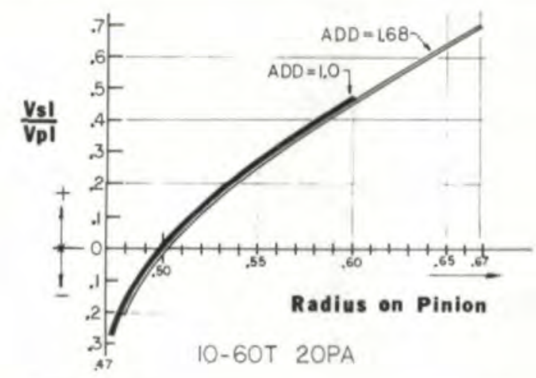

Fig. 22

(continued on page 48)

Involutometry Illustrations

Harlan W. Van Gerpen, P.E.
C. Kent Reece, P.E.
Van Gerpen-Reece Engineering, Cedar Falls, IA

In our last issue, the labels on the drawings illustrating "Involutometry" by Harlan Van Gerpen and C. Kent Reece were inadvertently omitted. For your convenience we have reproduced the corrected illustrations here. We regret any inconvenience this may have caused our readers.

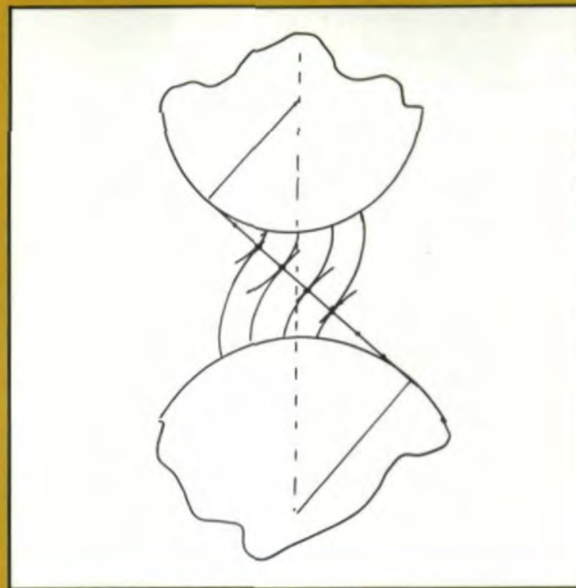

Fig. 3 – Multiple involute curves.

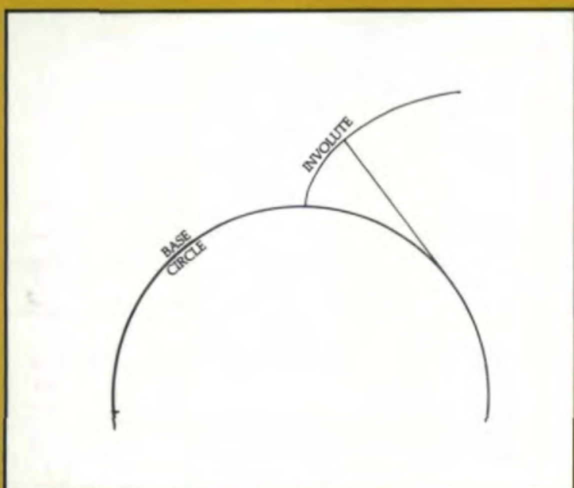

Fig. 1 – Involute curve.

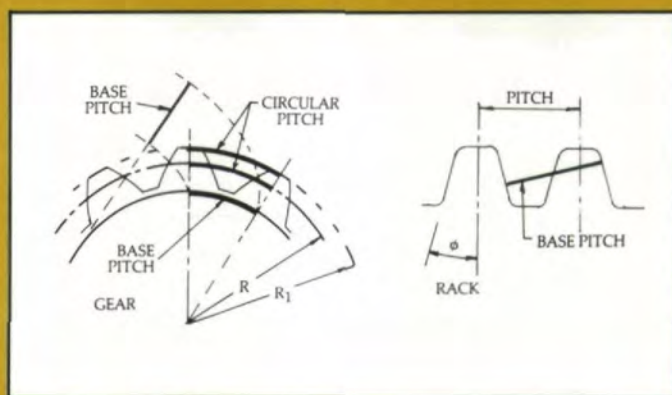

Fig. 4 – Base pitch of a gear and a rack.

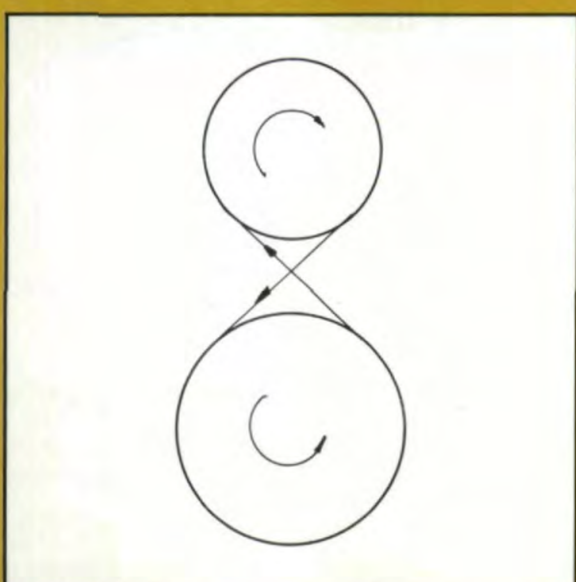

Fig. 2 – Crossed belt drive.

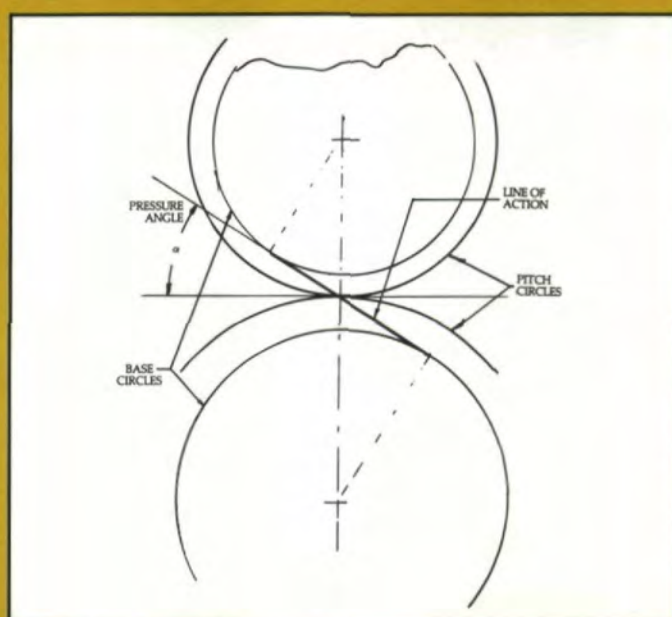

Fig. 5 – Line of action and pressure angle.

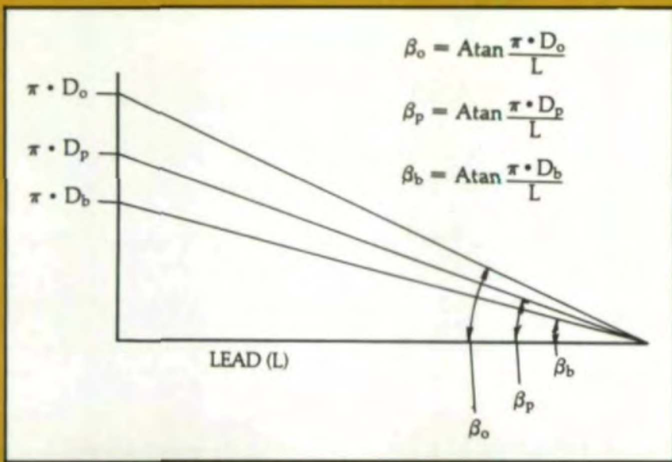

Fig. 6—Diagram to illustrate helix angle variation.

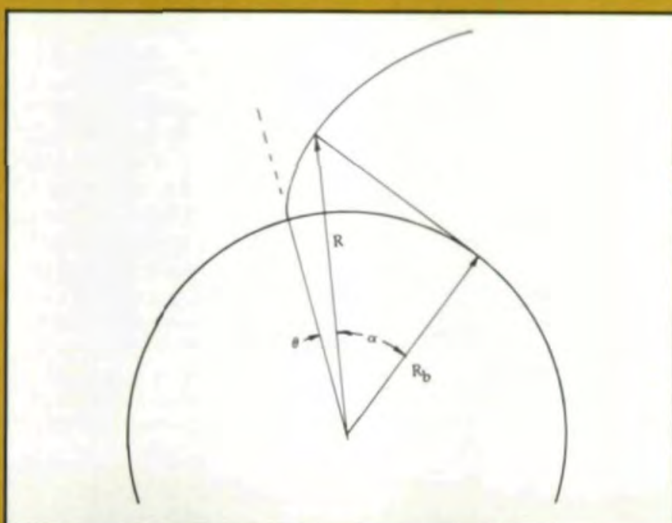

Eq. 2

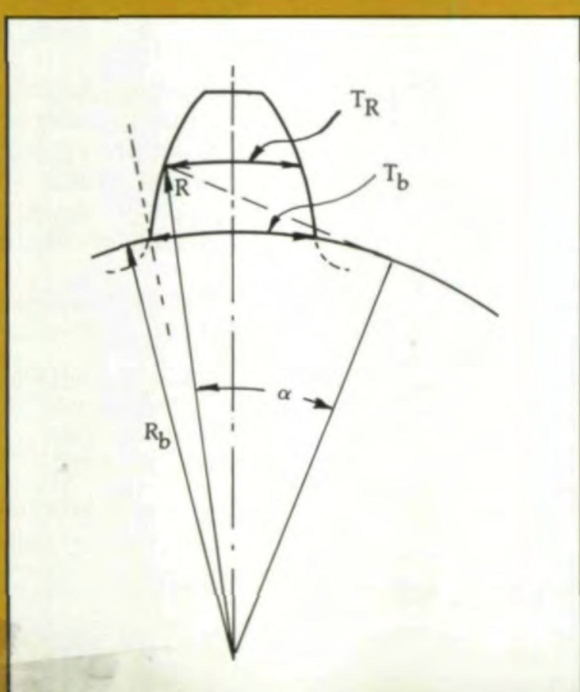

Eq. 3

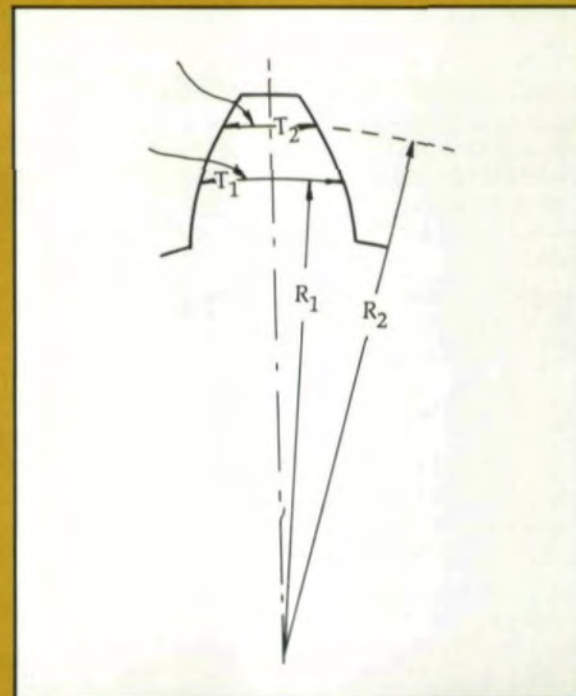

Eq. 4

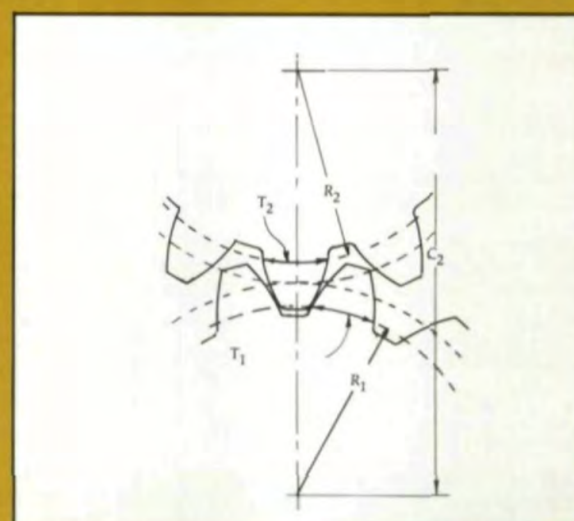

Eq. 13

Eq. 14

CLASSIFIED

Rates: Classified Display—per inch (minimum 3) **1X**-$130, **3X**-$120, **6X**-$110. Type will be set to advertiser's layout or *Gear Technology* will set type at no extra charge. **Word Count:** 35 characters per line, 7 lines per inch.

Payment: Full payment must accompany classified ads. Mail copy to *Gear Technology,* P.O. Box 1426, Elk Grove Village, IL 60009. **Agency Commission:** No agency commission on classifieds.

Material Deadline: Ads must be received by the 25th of the month, two months prior to publication. **Acceptance:** Publisher reserves the right to accept or reject classified advertisements at his discretion.

COMPUTER AIDS

GEAR ESTIMATING

The COSTIMATOR® computer *aided cost estimating system insures* speed and consistency in the difficult task of estimating the costs of all types of gears.

Used by small shops and Fortune 500 companies throughout the country.

For complete information contact us today.

Manufacturers Technologies, Inc.
59G Interstate Dr.
West Springfield, MA 01089
(413) 733-1972

CIRCLE A-27 ON READER REPLY CARD

GEAR CALCULATION PROGRAMS FOR THE GEAR MANUFACTURER

INEXPENSIVE, EASY TO RUN ON IBM COMPATIBLES

EXTERNAL — INCH (DP)
INTERNAL — METRIC (Mod.)
SPUR
HELICAL

STRAIGHT BEVEL (104)
SPIRAL BEVEL #16 & 27 GRD
BLANK AND SUMMARIES

For Brochure and More Information
CALL OR WRITE
UNIVERSAL GEAR CO. INC.
P.O.Box A.G., Anza, CA 92306
(714) 763-4616

CIRCLE A-33 ON READER REPLY CARD

GEARTECH *Software, Inc.*

GEAR DESIGN/ANALYSIS for IBM PC & compatibles. GEARCALC ($995): design optimum spur & helical gearsets from application data. AGMA218 ($1495): calculate pitting and bending fatigue lives per AGMA Std. 218.01. SCORING+ ($495): analyze/plot scoring & wear probabilities. Fast, menu-driven programs work as one system (combined price $2495), do extensive error-checking. Comprehensive manuals (theory, operation, examples) included. Demo available. GEARTECH Software, Inc., 1017 Pomona Ave., Albany, CA 94706 (415) 524-0668.

CIRCLE A-35 ON READER REPLY CARD

COMPUTER AIDS

GEARS SPLINES

DESIGN & TOOLING CONSULTING & SOFTWARE

- Let us design your gears for greater strength.
- Let us install our software and train your people in the latest gear and cutter computing methods. Trial periods available.
- You can benefit from our many years of experience with computers, gear design and manufacturing.
- Software for IBM and compatible computers.

VAN GERPEN-REECE ENGINEERING
1502 Grand Blvd.
Cedar Falls, Iowa 50613
(319) 266-4674

CIRCLE A-34 ON READER REPLY CARD

GEAR

DESIGN ANALYSIS
IBM COMPATIBLE COMPUTERS
WORM • SPUR • HELICAL • INTERNAL

- Source Code Provided (Basic)
- Self Prompting
- Complete Instruction Manuals
- Non-Standard Center Distances
- Recess Designs
- Non-Standard Tooth Depths
- Contact Diagram for Worm Drives
- Tolerances per AGMA 390.03

LOAD ANALYSIS per

- Buckingham Equations
- AGMA 218.01 or 440.04 for WORMS
- Buckingham Gear Books Available

BUCKINGHAM ASSOCIATES INC.
Springfield, VT 05156

CIRCLE A-23 ON READER REPLY CARD

BUSINESS OPPORTUNITY

. . . FOR GEAR CONSULTANTS

Put EXCITING NEW GEAR DIAGNOSTIC TECHNOLOGY to work solving your clients' most critical gear problems.

Fortune 500s are now getting BREAKTHROUGH ENHANCEMENTS IN MONITORING GEAR PERFORMANCE AND CONDITION . . . for end of line (QA), predictive maintenance & engineering and testing applications.

Join MTC in applying this technology. Call ED PAGE for more information.

MONITORING TECHNOLOGY CORPORATION
2779 Hartland Road
Falls Church, VA 22043
Call (703) 698-5520

CIRCLE A-28 ON READER REPLY CARD

Bring in new customers for your business by advertising in *GEAR TECHNOLOGY,* The Journal of Gear Manufacturing.
Call (312) 437-6604

BACK TO BASICS . . .
(continued from page 43)
and flank of the gear that must pass over each other.

Fig. 22 is a plot of the ratio of the sliding velocity and the rotational velocity at various radii on the pinion for a standard addendum and a 1.68 long addendum. The oversize has a significant effect on the pinion tip with the involute sliding approaching 70% of the pitch line velocity for the long addendum design.

Very Small Pinions

Seeing just how small a number of teeth can be designed into the pinion of a gear set is not only a challenge, but also a practical exercise. Reduced numbers of gear pairs can reduce the number of components needed as well as cost and space requirements. In the case of a reversing drive, a one-pair set can reduce the cumulative effect of total backlash. However, other matters involved require careful consideration before using such small pinions. Gear manufacturers will warn of the difficulties in producing such parts with useable profiles, especially in the region near the base circle.

Earle Buckingham found a design for a five tooth spur gear set, but concluded that a 22.5° pressure angle was required.[1] He found a symmetrical rack form would work and described the design in one of his books. This pinion is shown in Fig. 23. It has a contact ratio of 1.06 available.

Spur pinions of four teeth have also been made. One such example is presented in Fig. 24. This design uses and requires an unsymmetrical basic rack, implying a separate generating tool for the pinion and the gear. It is geometrically impossible to develop any spur pinions with sufficient involute form to get a contact ratio equal to 1.0 with fewer than four teeth.

If helical gears are considered, it is possible to make and use pinions of one, two and three teeth, and a sketch is given in Fig. 25 of a one-tooth helical pinion to show the possibilities.

References

1. BUCKINGHAM, EARLE. *Spur Gear Design, Operation and Production.* 1st ed. New York: McGraw-Hill, 1928. p. 194.

Acknowledgement: *Presented at SME Gear Processing and Manufacturing Clinic, 1987. Reprinted courtesy of Society of Manufacturing Engineers.*

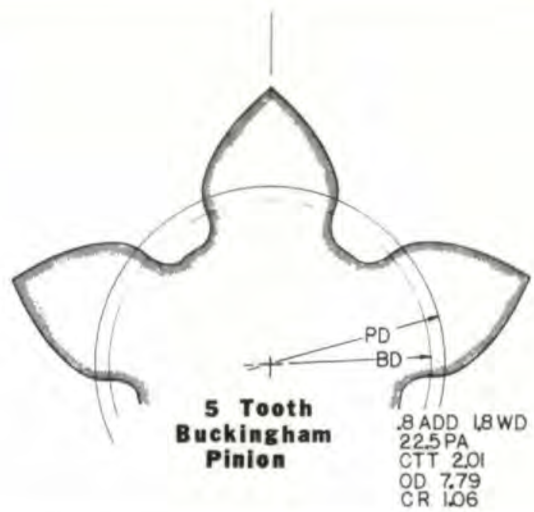

Fig. 23

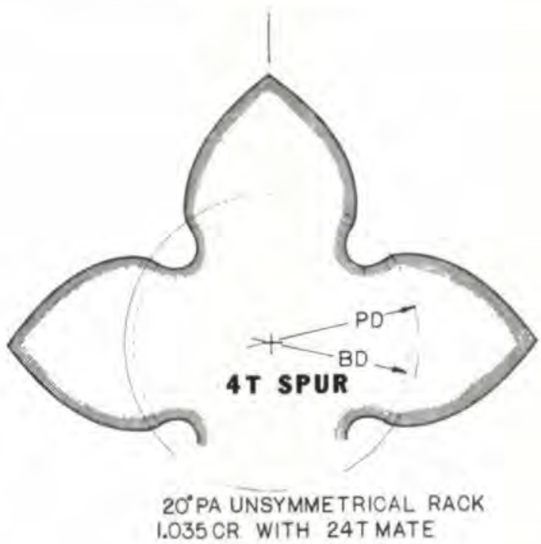

Fig. 24

Fig. 25